

Article

Not peer-reviewed version

Similarity Laws of Geometric and Material Distortion for Anisotropic Elastic Structure Subjected to Impact Loads

[Shuai Wang](#)^{*}, Xinzhe Chang, Fei Xu, Jicheng Li, Jiayi Wang

Posted Date: 3 March 2023

doi: 10.20944/preprints202303.0068.v1

Keywords: Similarity; Scaling; Geometric distortion; Anisotropic elastic materials; Structural impact



Preprints.org is a free multidiscipline platform providing preprint service that is dedicated to making early versions of research outputs permanently available and citable. Preprints posted at Preprints.org appear in Web of Science, Crossref, Google Scholar, Scilit, Europe PMC.

Copyright: This is an open access article distributed under the Creative Commons Attribution License which permits unrestricted use, distribution, and reproduction in any medium, provided the original work is properly cited.

Article

Similarity Laws of Geometric and Material Distortion for Anisotropic Elastic Structure Subjected to Impact Loads

Shuai Wang ^{a,b,c,*}, Xinzhe Chang ^a, Fei Xu ^{a,*}, Jicheng Li ^{b,c} and Jiayi Wang ^a

^a Institute for Computational Mechanics and Its Applications, Northwestern Polytechnical University, Xi'an 710072, Shaanxi, China;

^b Institute of Systems Engineering, China Academy of Engineering Physics, Mianyang, Sichuan 621999, China;

^c Shock and Vibration of Engineering Materials and Structures Key Laboratory of Sichuan Province, Mianyang, Sichuan 621999, China.

* Correspondence: wangsh2018@mail.nwpu.edu.cn; xufe@nwpu.edu.cn

Abstract: Although the similarity laws were widely used in impact fields, the scaling relations of anisotropic elastic structures often were broken when the geometric distortion (not equal scaling in different spatial directions) and the material distortion (different materials used for scaled model and full-size prototype) were considered. To overcome the difficulty of geometric and material distortion, a directional framework of similarity laws, termed as oriented-density-length-velocity (ODLV) system, is proposed for the anisotropic elastic structure under impact loads. Different from previous similarity law systems using scalar dimensional analysis, the directional similarity law framework mainly considers spatial anisotropy for structural geometry and material parameters. Based on the oriented dimensional analysis and the orthotropic Hooke's law, directional dimensionless numbers and directional scaling relations with geometric power properties for the elastic modulus and the Poisson's ratio are presented systematically. By selecting the dominant material parameters controlling similarity, three important scaling techniques with correction of geometric width and thickness are proposed to compensate for the difficulty of distortion. A clamped square plate with different anisotropic and isotropic elastic materials subjected to dynamic pressure pulse is verified numerically and discussed in detail. The results show that the thin square plate prototype must be scaled to be the thinner/thicker rectangular plate, and the components of displacement, stress and strain between scaled model and full-scale prototype behave good consistency in both spatial and temporal fields.

Keywords: similarity; scaling; geometric distortion; anisotropic elastic materials; structural impact

1. Introduction

Due to impractical, high cost, limited experimental facilities and other reasons, it was often not feasible to conduct full-size experimental studies on impacted structures [1]. In this case, it was very attractive to develop the scaling methods using scaled model instead of full-size prototype in experimental research. The method relating physical quantities between the scaled model and the full-size prototype was called to be similarity laws [1,2], which was usually based on the similar premise of geometry, materials and loads. With the development of impact dynamics, scaled models had been extensively applied in many fields of structural impact, no matter for the isotropic solid materials or advanced anisotropic composite materials [3,4]. In contrast, the similarity laws of anisotropic materials are more complicated because the material parameters are closely related to directivity of structural geometry space.

The traditional similarity laws were well-known and based on a basic geometric scaling factor relating any spatial directions and material parameters [1,2]. The geometric scaling factor was defined as $\beta = L_m/L_p$, where L was the characteristic length of the structure; the subscripts m and p represented scaled model and full-size prototype, respectively. In addition, it was used not only for the scaling test of isotropic materials [1,2], but also for the scaling test of more complex anisotropic

composites [5–8]. However, the traditional similarity laws do not allow the distortion problem in which the input parameters such as materials and geometry cannot fully satisfy the requirements of the scaling relations. The material distortion is usually caused by the material strain rate effects, the fracture and the use of different materials for scaled model and full-size prototype, while the geometric distortion is usually caused by different geometric scaling factors in different spatial directions [1]. Within a few decades of the initial development of the similarity laws of structural impact, the material and geometric distortions have been considered difficult to overcome whether for both isotropic [1] or anisotropic materials [9].

Because of the widespread existence of the material and geometric distortion, the application of traditional similarity laws has been seriously limited [10–13]. For example, different materials must be used in a scaled model because the completely same materials as the prototype cannot be found. Another example was that the geometry of the structures cannot be manufactured efficiently, especially in the thickness directions of scaled models. To solve the difficulty of distortion of metal materials, in the last two decades, some researchers extended the traditional similarity laws by using a new scaling relation with the basic scaling factor of length, density and velocity [13–18] and reasonably designing the optimal similitude materials [19,20]. On this basis, the initial conditions (impact velocity and density/mass) of the scaled model were corrected to compensate for distortion of different materials with strain hardening, strain-rate sensitive and thermal effects. Some studies further considered the influence of geometric distortion of thickness and obtained the simple scaling relations by empirical iterate methods [21–23] and by dimensionless analysis method for impacted simple beam and plate [24]. Since the defects of traditional similarity laws were overcome fundamentally, these works established a new scaling system and had gradually become widely used in the last twenty years [20]. However, the new similarity laws have not been applied to study the impact problem of anisotropic materials due to its complexity.

With the development of science and technology, anisotropic materials represented by composite materials are widely used in aircraft structures and other engineering fields [25]. The essential difficulty of anisotropic material similarity is that the material parameters were closely related to the different spatial orientations. In order to consider directivity of space, Wang et al. [26] proposed a directional similarity framework based on the oriented dimensional analysis method and the impacted thin-plate model. Since three directions of space were introduced into the bases of dimensional analysis, the similarity of geometric distortion including all stress, strain and displacement components were expressed systematically. However, due to the limitation of the research subjects of the isotropic plastic materials, this work only considered the thickness distortion and ignored the inherent capability of width distortion. Based on the framework, Li et al. [27] further expanded the application scope to obtain the similarity of isotropic elastic-plastic coupling situation. Meanwhile, Davey et al. [28] developed a scaling system with width and thickness distortion for isotropic and anisotropic elastic materials based on equation analysis method. When dynamic loading involved a dominant component of velocity/displacement, different anisotropic and isotropic elastic materials can obtain approximate similarity. Nevertheless, this work did not carry out in-depth and systematic analysis on the anisotropic material and geometrical distortion, and only used two stiffness coefficients in the x direction and the x - y plane direction as the dominant material parameters to obtain incomplete similarity of some physical quantities.

The main defect of the previous similarity laws to solve distortion problem was that they only focused on isotropic materials and rarely studied from the perspective of anisotropic materials. The essential reason was that, in the dimension and similarity analysis, most of them did not take into account the directivity of structural characteristic length and material parameters. In order to study the anisotropic similarity laws with material and geometric distortion more systematically and deeply, in this paper, a distorted similarity law framework of anisotropic elasticity was proposed by extending the directional similarity framework proposed in Ref. [26]. Compared with the previous other similarity laws, the new similarity laws were based on dimensional analysis and the classical plate theory, so it was very simple and understandable. More importantly, by using three spatial characteristic lengths instead of the traditional one in dimensional analysis of anisotropic elastic

materials, the directivity of physical quantities and structural geometric characteristics were systematically introduced into dimensionless numbers and scaling relations. The applicability and mechanism of the material and geometric distortion of anisotropic elasticity were also deeply explored.

In what follows, Section 2 introduces our newly proposed scaling procedure for material and geometric distortion of anisotropic elasticity. Section 3 investigates the numerical models of a clamped square plate of anisotropic elasticity subjected to dynamic pressure pulse. Section 4 discusses in depth the similarity mechanism caused by material parameters. Section 5 summarizes this work.

2. Distorted scaling procedure of anisotropic elasticity

2.1. The main defects of the previous similarity laws

In the past, the similarity laws to solve distortion problem mainly focused on the plastic materials with strain hardening, strain rate and temperature effects, but rarely dealt with the anisotropic elastic problem under impact. When scaled model was used for different anisotropic elastic materials and the geometric distorted structures, the previous similarity methods were broken because the anisotropic elastic parameters were closely related to the spatial direction. The dissimilar phenomena are briefly analyzed as follows.

Considering that the elastic modulus E_{ij} and the Poisson's ratio ν_{ij} are the dominant similar parameters for anisotropic materials, their general dimensions are expressed as $\dim(E_{ij}) = \text{ML}^{-1}\text{T}^{-2}$ and $\dim(\nu_{ij}) = 1$, where the notation ' $\dim(\cdot)$ ' represents dimension of physical quantity; the symbols L , M and T represent dimensions of length, mass, and time, respectively; and $i, j = x, y, z$. The well-known Buckingham theorem [1] states that physical quantities of a mechanical model can be reduced to dimensionless numbers to simplify causal relationship between them. When the density ρ , the characteristic length \bar{L} and the velocity V are used as bases of dimensional analysis [18], the dimensionless numbers $\Pi_{E_{ij}} = [\rho V^2 / E_{ij}]$ and $\Pi_{\nu_{ij}} = [\nu_{ij}]$ can be obtained. The number $\Pi_{E_{ij}}$, often termed as the Cauchy number [29], is a well-known important dimensionless number and control the similarity of elasticity, while the number $\Pi_{\nu_{ij}}$ is a natural dimensionless number. For scaled model and prototype, the dimensionless equality $[\rho_m V_m^2 / (E_{ij})_m] = [\rho_p V_p^2 / (E_{ij})_p]$ and $[(\nu_{ij})_m] = [(\nu_{ij})_p]$ can be translated into the scaling relations $\beta_{E_{ij}} = \beta_\rho \beta_V^2$ and $\beta_{\nu_{ij}} = 1$, respectively. The two scaling relations indicate that the necessary condition of similarity of anisotropic elastic materials is that the material parameters in each direction satisfy the same scaling factor. Therefore, when the material used in the scaled model is different from that of the prototype, the similarity condition will be broken. In addition, since the scaling relation of the Poisson's ratio in each direction is equal to 1, it can be inferred that another necessary condition of similarity is that the scaled model is geometrically similar to the full-size prototype. Thus, when the geometric characteristics of the structure in different directions are scaled according to different scaling factors, the similarity condition will also be broken.

The above analysis shows that similarity laws of the anisotropic material and geometrical distortion cannot be derived when the general dimensional analysis is used. In order to overcome this difficulty essentially, we further consider the directional similarity law framework.

2.2. Review of the directional framework of similarity laws

Different from the general dimensional analysis, which used one scalar length dimension L for all the structural characteristic length \bar{L} , the directional framework of similarity laws used the oriented length dimensions L_x , L_y and L_z [30,31] for three spatial characteristic lengths \bar{L}_x , \bar{L}_y and \bar{L}_z , respectively. The advantage of oriented dimension was that it introduced spatial directionality into dimensional analysis through different characteristic lengths. To determine the oriented dimensions of structural impact, a mechanical model of a thin-plate impact problem was further used, as shown in Figure 1. The main reason for using the thin-plate impact model was that

its loads and displacements were dominated by transverse components, thus reducing the complexity of oriented dimensional analysis. For the classical plate theory, the strain components [31] were simplified as $\varepsilon_x = \left(\frac{\partial u}{\partial x}\right) + \frac{1}{2}\left(\frac{\partial w}{\partial x}\right)^2 - \left(Z_0 \frac{\partial^2 w}{\partial x^2}\right)$, $\varepsilon_y = \left(\frac{\partial v}{\partial y}\right) + \frac{1}{2}\left(\frac{\partial w}{\partial y}\right)^2 - \left(Z_0 \frac{\partial^2 w}{\partial y^2}\right)$, $\gamma_{xy} = \left(\frac{\partial u}{\partial y} + \frac{\partial v}{\partial x}\right) + \left(\frac{\partial w}{\partial x} \frac{\partial w}{\partial y}\right) - \left(2Z_0 \frac{\partial^2 w}{\partial x \partial y}\right)$, $\gamma_{xz} = \left(-\frac{\partial w}{\partial x}\right) + \left(\frac{\partial w}{\partial x}\right) = 0$, $\gamma_{yz} = \left(-\frac{\partial w}{\partial y}\right) + \left(\frac{\partial w}{\partial y}\right) = 0$ and $\varepsilon_z = \left(\frac{\partial w}{\partial z}\right) = 0$, where u , v and w represented the displacement components of neutral plane elements on the x -axis, the y -axis and the z -axis, respectively; Z_0 represented the distance to the neutral plane. The whole displacement fields were expressed as $\delta_x = u - \left(Z_0 \frac{\partial w}{\partial x}\right)$, $\delta_y = v - \left(Z_0 \frac{\partial w}{\partial y}\right)$ and $\delta_z = w$, where the second term to the right of ε_x and ε_y represented the displacement caused by the deflection [31]. Based on this impact model and the oriented dimensional method, the directional similarity framework including oriented dimension, directional dimensionless number and directional scaling relations were derived as follows [26]:

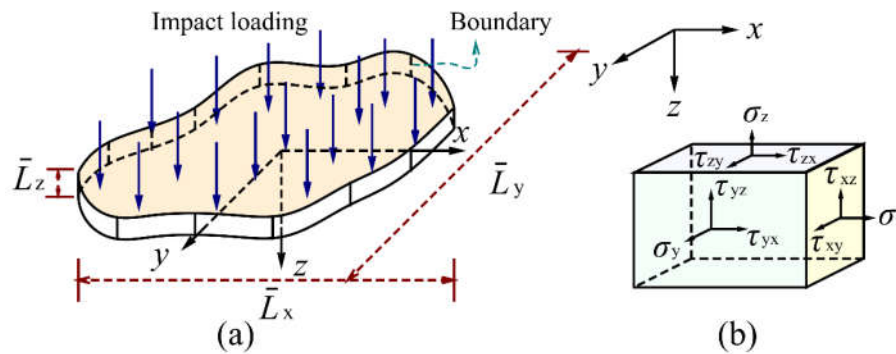


Figure 1. The thin-plate impact model. (a) a thin-plate subjected to impact loads; (b) the directivity of physical quantities.

When the oriented dimensional analysis method was used, the oriented dimensions of main physical quantities in the thin-plate impact problem can be obtained. For example, based on the equation of motion, $\sigma_{ij} + \frac{\partial \sigma_{ij}}{\partial x_k} dx_k = \rho \frac{\partial^2 u_k}{\partial t^2}$, the oriented analysis was given as $\dim(\sigma_{ij}) = \dim(\rho) \dim(u_k) / \dim(t)^2$, which can be derived the oriented dimension $\mathbb{L}_x \mathbb{L}_y^{-1} \mathbb{L}_z^{-1} \mathbb{M} \mathbb{T}^{-2}$, $\mathbb{L}_x^{-1} \mathbb{L}_y \mathbb{L}_z^{-1} \mathbb{M} \mathbb{T}^{-2}$, $\mathbb{L}_x^{-1} \mathbb{L}_y^{-1} \mathbb{L}_z \mathbb{M} \mathbb{T}^{-2}$, $\mathbb{L}_z^{-1} \mathbb{M} \mathbb{T}^{-2}$, $\mathbb{L}_y^{-1} \mathbb{M} \mathbb{T}^{-2}$ and $\mathbb{L}_x^{-1} \mathbb{M} \mathbb{T}^{-2}$ for the stress components σ_x , σ_y , σ_z , τ_{xy} , τ_{xz} and τ_{yz} , respectively. Similarly, based on the oriented analysis of the strain components, the displacement fields of the classical plate theory and the impact loads, the oriented dimensions of 6 strain components, 3 displacement components, impact mass and pulse pressure can also be derived. The detailed derivation can be found in Ref. [26]. The main physical quantities and their corresponding oriented dimensions in the thin-plate impact problem are listed in Table 1. Compared with the scalar dimensions such as $\dim(\sigma_{ij}) = \mathbb{L} \mathbb{M} \mathbb{T}^{-2}$ and $\dim(\varepsilon_{ij}) = 1$, the oriented dimensions can effectively distinguish physical quantities in different directions, especially originally dimensionless strains. In addition, Ref. [26] also defined the oriented dimensions of equivalent stress, equivalent strain and plastic strain components. Since the study object in this paper is anisotropic elasticity, the oriented expressions involving plasticity are not listed in here and later.

Table 1. Oriented dimensions of physical quantity in the thin-plate impact problem.

Physical quantity	Dimension	Physical quantity	Dimension
Density ρ	$\mathbb{M} \mathbb{L}_x^{-1} \mathbb{L}_y^{-1} \mathbb{L}_z^{-1}$	Strain ε_y	$\mathbb{L}_y^{-2} \mathbb{L}_z^2$
Length \bar{L}_x	\mathbb{L}_x	Strain γ_{xy}	$\mathbb{L}_x^{-1} \mathbb{L}_y^{-1} \mathbb{L}_z^2$
Length \bar{L}_y	\mathbb{L}_y	Strain ε_z	1
Length \bar{L}_z	\mathbb{L}_z	Strain γ_{xz}	$\mathbb{L}_x^{-1} \mathbb{L}_z$
Velocity V_z	$\mathbb{L}_z \mathbb{T}^{-1}$	Strain γ_{yz}	$\mathbb{L}_y^{-1} \mathbb{L}_z$
Stress σ_x	$\mathbb{L}_x \mathbb{L}_y^{-1} \mathbb{L}_z^{-1} \mathbb{M} \mathbb{T}^{-2}$	Time t	\mathbb{T}
Stress σ_y	$\mathbb{L}_x^{-1} \mathbb{L}_y \mathbb{L}_z^{-1} \mathbb{M} \mathbb{T}^{-2}$	Displacement δ_x	$\mathbb{L}_x^{-1} \mathbb{L}_z^2$

Stress σ_z	$\mathbb{L}_x^{-1}\mathbb{L}_y^{-1}\mathbb{L}_z\mathbb{M}\mathbb{T}^{-2}$	Displacement δ_y	$\mathbb{L}_y^{-1}\mathbb{L}_z^2$
Stress τ_{xy}	$\mathbb{L}_z^{-1}\mathbb{M}\mathbb{T}^{-2}$	Displacement δ_z	\mathbb{L}_z
Stress τ_{xz}	$\mathbb{L}_y^{-1}\mathbb{M}\mathbb{T}^{-2}$	Impact mass G	\mathbb{M}
Stress τ_{yz}	$\mathbb{L}_x^{-1}\mathbb{M}\mathbb{T}^{-2}$	Impulse pressure P_z	$\mathbb{L}_x^{-1}\mathbb{L}_y^{-1}\mathbb{L}_z\mathbb{M}\mathbb{T}^{-2}$
Strain ε_x	$\mathbb{L}_x^{-2}\mathbb{L}_z^2$		

When the density ρ , the characteristic length \bar{L}_x , \bar{L}_y , \bar{L}_z and the velocity V_z are selected as bases of dimensional analysis, according to the Buckingham theorem [1], 23 physical quantities in Table 1 can be casted as the following 18 dimensionless numbers:

- six stress components

$$\Pi_{\sigma_x} = \left[\frac{\rho V_z^2}{\sigma_x} \left(\frac{\bar{L}_x}{\bar{L}_z} \right)^2 \right], \Pi_{\sigma_y} = \left[\frac{\rho V_z^2}{\sigma_y} \left(\frac{\bar{L}_y}{\bar{L}_z} \right)^2 \right], \Pi_{\tau_{xy}} = \left[\frac{\rho V_z^2}{\tau_{xy}} \left(\frac{\sqrt{\bar{L}_x \bar{L}_y}}{\bar{L}_z} \right)^2 \right], \Pi_{\sigma_z} = \left[\frac{\rho V_z^2}{\sigma_z} \right],$$

$$\Pi_{\tau_{xz}} = \left[\frac{\rho V_z^2}{\tau_{xz}} \left(\frac{\bar{L}_x}{\bar{L}_z} \right) \right], \Pi_{\tau_{yz}} = \left[\frac{\rho V_z^2}{\tau_{yz}} \left(\frac{\bar{L}_y}{\bar{L}_z} \right) \right];$$
(1a-f)

- six strain components

$$\Pi_{\varepsilon_x} = \left[\varepsilon_x \left(\frac{\bar{L}_x}{\bar{L}_z} \right)^2 \right], \Pi_{\varepsilon_y} = \left[\varepsilon_y \left(\frac{\bar{L}_y}{\bar{L}_z} \right)^2 \right], \Pi_{\gamma_{xy}} = \left[\gamma_{xy} \left(\frac{\sqrt{\bar{L}_x \bar{L}_y}}{\bar{L}_z} \right)^2 \right], \Pi_{\varepsilon_z} = [\varepsilon_z],$$

$$\Pi_{\gamma_{xz}} = \left[\gamma_{xz} \left(\frac{\bar{L}_x}{\bar{L}_z} \right) \right], \Pi_{\gamma_{yz}} = \left[\gamma_{yz} \left(\frac{\bar{L}_y}{\bar{L}_z} \right) \right];$$
(2a-f)

- three displacement components

$$\Pi_{\delta_x} = \left[\frac{\delta_x}{\bar{L}_x} \left(\frac{\bar{L}_x}{\bar{L}_z} \right)^2 \right], \Pi_{\delta_y} = \left[\frac{\delta_y}{\bar{L}_y} \left(\frac{\bar{L}_y}{\bar{L}_z} \right)^2 \right], \Pi_{\delta_z} = \left[\frac{\delta_z}{\bar{L}_z} \right];$$
(3a-c)

- time, impact mass and impulse pressure

$$\Pi_t = \left[\frac{t V_z}{\bar{L}_z} \right]; \Pi_G = \left[\frac{M}{\rho (\bar{L}_x \bar{L}_y \bar{L}_z)} \right]; \Pi_{P_z} = \left[\frac{P_z}{\rho V_z^2} \right].$$
(4a-c)

It should be noted that Eq. (1a-f), Eq. (2a-f) and Eq. (3a-c) can be expressed as the three tensor forms $\Pi_{\sigma_{ij}} = \frac{\rho V_z^2}{\sigma_{ij}} \left(\sqrt{\bar{L}_i \bar{L}_j} / \bar{L}_z \right)^2$, $\Pi_{\varepsilon_{ij}} = \varepsilon_{ij} \left(\sqrt{\bar{L}_i \bar{L}_j} / \bar{L}_z \right)^2$ and $\Pi_{\delta_i} = \frac{\delta_i}{\bar{L}_i} \left(\sqrt{\bar{L}_i \bar{L}_j} / \bar{L}_z \right)^2$ (no sum on i and j), where $i, j = x, y, z$. Apparently, the stress, strain and displacement components were all related to the structural characteristic length of three spatial directions in the dimensionless relationship, and had the characteristic form of geometric power law of $\left(\sqrt{\bar{L}_i \bar{L}_j} / \bar{L}_z \right)^2$. In contrast, these dimensionless numbers in scalar dimensional analysis [18] were expressed as $\Pi_{\sigma_{ij}} = \frac{\rho V_z^2}{\sigma_{ij}}$, $\Pi_{\varepsilon_{ij}} = \varepsilon_{ij}$ and $\Pi_{\delta_i} = \frac{\delta_i}{\bar{L}_i}$, which had no the characteristic of geometric power law.

Based on the above dimensionless numbers, the scaling relations of physical quantities were listed in Table 2. Obviously, these similarity relations were based on expression of the five basic factors β_ρ , $\beta_{\bar{L}_x}$, $\beta_{\bar{L}_y}$, $\beta_{\bar{L}_z}$ and β_{V_z} , which behaved quite differently from the previous similitude laws using only a single geometric scaling factor β (i.e., $\beta_{\bar{L}_x} = \beta_{\bar{L}_y} = \beta_{\bar{L}_z} = \beta$). Thus, when any two of $\beta_{\bar{L}_x}$, $\beta_{\bar{L}_y}$ and $\beta_{\bar{L}_z}$ was not equal, the similarity laws were geometrically distorted.

Table 2. Main scaling relations of structural impact in the ODLV system.

Variable	Scaling factor	Variable	Scaling factor
Length \bar{L}_x	$\beta_{\bar{L}_x} = (\bar{L}_x)_m / (\bar{L}_x)_p$	Strain ε_y	$\beta_{\varepsilon_y} = (\beta_{\bar{L}_z} / \beta_{\bar{L}_y})^2$
Length \bar{L}_y	$\beta_{\bar{L}_y} = (\bar{L}_y)_m / (\bar{L}_y)_p$	Strain γ_{xy}	$\beta_{\gamma_{xy}} = \left(\beta_{\bar{L}_z} / \sqrt{\beta_{\bar{L}_x} \beta_{\bar{L}_y}} \right)^2$
Length \bar{L}_z	$\beta_{\bar{L}_z} = (\bar{L}_z)_m / (\bar{L}_z)_p$	Strain ε_z	$\beta_{\varepsilon_z} = 1$
Density ρ	$\beta_\rho = \rho_m / \rho_p$	Strain γ_{xz}	$\beta_{\gamma_{xz}} = (\beta_{\bar{L}_z} / \beta_{\bar{L}_x})$
Velocity V_z	$\beta_{V_z} = (V_z)_m / (V_z)_p$	Strain γ_{yz}	$\beta_{\gamma_{yz}} = (\beta_{\bar{L}_z} / \beta_{\bar{L}_y})$
Stress σ_x	$\beta_{\sigma_x} = (\beta_\rho \beta_{V_z}^2) (\beta_{\bar{L}_x} / \beta_{\bar{L}_z})^2$	Time t	$\beta_t = (\beta_{\bar{L}_z} / \beta_{V_z})$
Stress σ_y	$\beta_{\sigma_y} = (\beta_\rho \beta_{V_z}^2) (\beta_{\bar{L}_y} / \beta_{\bar{L}_z})^2$	Displacement δ_x	$\beta_{\delta_x} = \beta_{\bar{L}_x} (\beta_{\bar{L}_z} / \beta_{\bar{L}_x})^2$
Stress σ_z	$\beta_{\sigma_z} = (\beta_\rho \beta_{V_z}^2)$	Displacement δ_y	$\beta_{\delta_y} = \beta_{\bar{L}_y} (\beta_{\bar{L}_z} / \beta_{\bar{L}_y})^2$
Stress τ_{xy}	$\beta_{\tau_{xy}} = (\beta_\rho \beta_{V_z}^2) \left(\frac{\sqrt{\beta_{\bar{L}_x} \beta_{\bar{L}_y}}}{\beta_{\bar{L}_z}} \right)^2$	Displacement δ_z	$\beta_{\delta_z} = \beta_{\bar{L}_z}$
Stress τ_{xz}	$\beta_{\tau_{xz}} = (\beta_\rho \beta_{V_z}^2) (\beta_{\bar{L}_x} / \beta_{\bar{L}_z})$	Impact mass M	$\beta_M = \beta_\rho (\beta_{\bar{L}_x} \beta_{\bar{L}_y} \beta_{\bar{L}_z})$
Stress τ_{yz}	$\beta_{\tau_{yz}} = (\beta_\rho \beta_{V_z}^2) (\beta_{\bar{L}_y} / \beta_{\bar{L}_z})$	Surface pressure P_z	$\beta_{P_z} = (\beta_\rho \beta_{V_z}^2)$
Strain ε_x	$\beta_{\varepsilon_x} = (\beta_{\bar{L}_z} / \beta_{\bar{L}_x})^2$		

The derivation above formed the basic framework of the directional similarity laws. Since it was based on the oriented-density-length-velocity bases of dimensional analysis, the above similarity laws were termed as the ODLV system.

2.3. Directional dimensionless number and scaling relations of anisotropic elasticity

In this section, we further extend the directional framework of ODLV to the impact problem when thin-plate is made of anisotropic elastic materials.

In order to derive the directional similarity laws of anisotropic elastic materials, the Hooke's law of orthotropic anisotropy [32],

$$\left. \begin{aligned} \varepsilon_x &= \frac{\sigma_x}{E_x} - \nu_{yx} \frac{\sigma_y}{E_y} - \nu_{zx} \frac{\sigma_z}{E_z}, & \varepsilon_y &= \frac{\sigma_y}{E_y} - \nu_{zy} \frac{\sigma_z}{E_z} - \nu_{xy} \frac{\sigma_x}{E_x} \\ \varepsilon_z &= \frac{\sigma_z}{E_z} - \nu_{xz} \frac{\sigma_x}{E_x} - \nu_{yz} \frac{\sigma_y}{E_y}, & \gamma_{xy} &= \frac{\tau_{xy}}{G_{xy}}, & \gamma_{xz} &= \frac{\tau_{xz}}{G_{xz}}, & \gamma_{yz} &= \frac{\tau_{yz}}{G_{yz}} \end{aligned} \right\}, \quad (5a-f)$$

are studied, where $\nu_{ij} = |\varepsilon_j / \varepsilon_i|$ is Poisson's ratio; E and G specifically refer to Young's modulus and shear modulus, respectively. According to symmetry of flexibility matrix, the material parameters have the reciprocal relations $\nu_{yx}/E_y = \nu_{xy}/E_x$, $\nu_{zx}/E_z = \nu_{xz}/E_x$ and $\nu_{zy}/E_z = \nu_{yz}/E_x$ [32]. Therefore, among these material parameters, only nine are independent of each other for anisotropic materials, namely, E_x , E_y , E_z , G_{xy} , G_{xz} , G_{yz} , ν_{xy} , ν_{xz} and ν_{yz} .

The oriented dimensional analysis of Eq. (5a-f) can obtain the following relation:

$$\left. \begin{aligned} \dim(E_x) &= \frac{\dim(\sigma_x)}{\dim(\varepsilon_x)}, \dim(E_y) = \frac{\dim(\sigma_y)}{\dim(\varepsilon_y)}, \dim(E_z) = \frac{\dim(\sigma_z)}{\dim(\varepsilon_z)} \\ \dim(G_{xy}) &= \frac{\dim(\tau_{xy})}{\dim(\gamma_{xy})}, \dim(G_{xz}) = \frac{\dim(\tau_{xz})}{\dim(\gamma_{xz})}, \dim(G_{yz}) = \frac{\dim(\tau_{yz})}{\dim(\gamma_{yz})} \\ \dim(\nu_{xy}) &= \frac{\dim(\varepsilon_y)}{\dim(\varepsilon_x)}, \dim(\nu_{xz}) = \frac{\dim(\sigma_y)}{\dim(\varepsilon_y)}, \dim(\nu_{yz}) = \frac{\dim(\sigma_z)}{\dim(\varepsilon_z)} \end{aligned} \right\} \quad (6a-i)$$

When the dimensions of stress and strain components in Table 1 are substituted into Eq. (6a-i), the oriented dimensions of elastic parameters can be derived, which are listed in Table 3. It is obvious that when the method of oriented dimensional analysis is used, the elastic parameters in different directions exhibit different dimensions, and the Poisson's ratio is no longer a dimensionless quantity.

Table 3. Oriented dimensions of elastic parameters in the ODLV system.

Physical quantity	Dimension	Physical quantity	Dimension
Elastic modulus, E_x	$\mathbb{L}_x^3 \mathbb{L}_y^{-1} \mathbb{L}_z^{-3} \mathbb{M} \mathbb{T}^{-2}$	Shear modulus, G_{yz}	$\mathbb{L}_x^{-1} \mathbb{L}_y \mathbb{L}_z^{-1} \mathbb{M} \mathbb{T}^{-2}$
Elastic modulus, E_y	$\mathbb{L}_x^{-1} \mathbb{L}_y^3 \mathbb{L}_z^{-3} \mathbb{M} \mathbb{T}^{-2}$	Poisson's ratio, ν_{xy}	$\mathbb{L}_x^2 \mathbb{L}_y^{-2}$
Elastic modulus, E_z	$\mathbb{L}_x^{-1} \mathbb{L}_y^{-1} \mathbb{L}_z \mathbb{M} \mathbb{T}^{-2}$	Poisson's ratio, ν_{xz}	$\mathbb{L}_x^2 \mathbb{L}_z^{-2}$
Shear modulus, G_{xy}	$\mathbb{L}_x \mathbb{L}_y \mathbb{L}_z^3 \mathbb{M} \mathbb{T}^{-2}$	Poisson's ratio, ν_{yz}	$\mathbb{L}_y^2 \mathbb{L}_z^{-2}$
Shear modulus, G_{xz}	$\mathbb{L}_x \mathbb{L}_y^{-1} \mathbb{L}_z^{-1} \mathbb{M} \mathbb{T}^{-2}$		

When the bases of ρ , \bar{L}_x , \bar{L}_y , \bar{L}_z and V_z are used, according to the Buckingham Π theorem, the elastic parameters in Table 3 can be deduced as the following dimensionless numbers:

- Elasticity modulus

$$\begin{aligned} \Pi_{E_x} &= \left[\frac{\rho V_z^2}{E_x} \left(\frac{\bar{L}_x}{\bar{L}_z} \right)^4 \right], \Pi_{E_y} = \left[\frac{\rho V_z^2}{E_y} \left(\frac{\bar{L}_y}{\bar{L}_z} \right)^4 \right], \Pi_{G_{xy}} = \left[\frac{\rho V_z^2}{G_{xy}} \left(\frac{\sqrt{\bar{L}_x \bar{L}_y}}{\bar{L}_z} \right)^4 \right], \\ \Pi_{E_z} &= \left[\frac{\rho V_z^2}{E_z} \right], \Pi_{G_{xz}} = \left[\frac{\rho V_z^2}{G_{xz}} \left(\frac{\bar{L}_x}{\bar{L}_z} \right)^2 \right], \Pi_{G_{yz}} = \left[\frac{\rho V_z^2}{G_{yz}} \left(\frac{\bar{L}_y}{\bar{L}_z} \right)^2 \right]; \end{aligned} \quad (7a-f)$$

- Poisson's ratio

$$\Pi_{\nu_{xy}} = \left[\nu_{xy} \left(\frac{\bar{L}_y}{\bar{L}_x} \right)^2 \right], \Pi_{\nu_{xz}} = \left[\nu_{xz} \left(\frac{\bar{L}_z}{\bar{L}_x} \right)^2 \right], \Pi_{\nu_{yz}} = \left[\nu_{yz} \left(\frac{\bar{L}_z}{\bar{L}_y} \right)^2 \right]. \quad (8a-c)$$

In the derivation above, the x-axis and y-axis directions of the characteristic length are consistent with the two main directions 11 and 22 of the material, respectively. Therefore, for anisotropic materials with ply angle, the selection of characteristic lengths is determined by the directions of materials rather than usual geometrical characteristics. In addition, Eqs. (7a-f) and (8a-c) can be expressed as the tensor forms $\Pi_{E_{ij}} = \left[\frac{\rho V_z^2}{E_{ij}} \left(\sqrt{\bar{L}_i \bar{L}_j / \bar{L}_z} \right)^4 \right]$ and $\Pi_{\delta_i} = [\nu_{ij} (\bar{L}_j / \bar{L}_i)^2]$ (no sum on i and j), respectively. Compared with the numbers $\Pi_{E_{ij}} = [\rho V^2 / E_{ij}]$ and $\Pi_{\nu_{ij}} = [\nu_{ij}]$ in scalar form, the new proposed dimensionless numbers here further express the geometrical characteristics of the structure by the geometric power term $\left(\sqrt{\bar{L}_i \bar{L}_j / \bar{L}_z} \right)^4$ and $(\bar{L}_j / \bar{L}_i)^2$.

When the directional dimensionless numbers of the elastic parameters are used for scaled model and full-size prototype, they can be further transformed into the scaling relations about materials. For the nine physical quantities in Table 3, their scaling relations are listed Table 4. The scaling

relations form a foundation of distortion scaling for anisotropic elasticity. Compared with the previous scaling relations $\beta_{E_{ij}} = \beta_\rho \beta_{\bar{V}_z}^2$ and $\beta_{\nu_{ij}} = 1$ in scalar dimensional analysis, the elastic parameters in different directions are closely related to the scaling of the characteristic length in the corresponding directions. When a scaled impact test is performed, the geometry, loads and material parameters of scaled model need to satisfy the relations in Table 2 and Table 4. After the test is completed, the behavior of the full-size prototype can be predicted from scaled model by using these relations.

Table 4. Scaling relations of elastic parameters in the ODLV system.

Variable	Scaling factor	Variable	Scaling factor
Elasticity modulus, E_x	$\beta_{E_x} = (\beta_\rho \beta_{\bar{V}_z}^2) (\beta_{\bar{L}_x} / \beta_{\bar{L}_z})^4$	Shear modulus, G_{yz}	$\beta_{G_{yz}} = (\beta_\rho \beta_{\bar{V}_z}^2) (\beta_{\bar{L}_y} / \beta_{\bar{L}_z})^2$
Elasticity modulus, E_y	$\beta_{E_y} = (\beta_\rho \beta_{\bar{V}_z}^2) (\beta_{\bar{L}_y} / \beta_{\bar{L}_z})^4$	Poisson's ratio, ν_{xy}	$\beta_{\nu_{xy}} = (\beta_{\bar{L}_x} / \beta_{\bar{L}_y})^2$
Elasticity modulus, E_z	$\beta_{E_z} = (\beta_\rho \beta_{\bar{V}_z}^2)$	Poisson's ratio, ν_{xz}	$\beta_{\nu_{xz}} = (\beta_{\bar{L}_x} / \beta_{\bar{L}_z})^2$
Shear modulus, G_{xy}	$\beta_{G_{xy}} = (\beta_\rho \beta_{\bar{V}_z}^2) \left(\sqrt{\beta_{\bar{L}_x} \beta_{\bar{L}_y} / \beta_{\bar{L}_z}} \right)^4$	Poisson's ratio, ν_{yz}	$\beta_{\nu_{yz}} = (\beta_{\bar{L}_y} / \beta_{\bar{L}_z})^2$
Shear modulus, G_{xz}	$\beta_{G_{xz}} = (\beta_\rho \beta_{\bar{V}_z}^2) (\beta_{\bar{L}_x} / \beta_{\bar{L}_z})^2$		

2.4. Correction methods for geometric and material distortion of anisotropic elasticity

When the relations in Table 4 are used to perform the scaling test of impact problem, the nine independent material parameters E_x , E_y , E_z , G_{xy} , G_{xz} , G_{yz} , ν_{xy} , ν_{xz} and ν_{yz} need to be satisfied. It is easy to find that these parameters are not independent of each other at scaling, and they have the following equation

$$\frac{\beta_{G_{xy}}}{\sqrt{\beta_{E_x} \beta_{E_y}}} = \frac{\beta_{G_{xz}}}{\sqrt{\beta_{E_x} \beta_{E_z}}} = \frac{\beta_{G_{yz}}}{\sqrt{\beta_{E_y} \beta_{E_z}}} = \frac{\beta_{\nu_{xy}}}{\sqrt{\beta_{E_x} / \beta_{E_y}}} = \frac{\beta_{\nu_{xz}}}{\sqrt{\beta_{E_x} / \beta_{E_z}}} = \frac{\beta_{\nu_{yz}}}{\sqrt{\beta_{E_y} / \beta_{E_z}}} = 1. \quad (9)$$

In practice, Eq. (9) is fully satisfied when the scaled model and the full-size prototype use exactly the same anisotropic materials. In this case, $\beta_{E_x} = \beta_{E_y} = \beta_{E_z} = \beta_{E_{xy}} = \beta_{E_{xz}} = \beta_{E_{yz}} = \beta_{\nu_{xy}} = \beta_{\nu_{xz}} = \beta_{\nu_{yz}} = 1$ and $\beta_{\bar{L}_x} = \beta_{\bar{L}_y} = \beta_{\bar{L}_z}$. Therefore, for the same anisotropic material, the impact behavior follows the traditional similarity laws and cannot be allowed to scaling of material and geometric distortion.

In what follows, in order to further consider the material and geometric distortion using different anisotropic parameters, the incomplete scaling techniques that select some physical quantities as dominant parameters are used to break the similarity constraint of Eq. (9).

- **Only thickness distortion**

For the thin-plate impact problem, when the deformation conforms to the geometric nonlinearity assumption of small strains under moderate rotation of $10^\circ - 15^\circ$, the transverse strain and stress components can be approximately ignored [26]. Then, the Hooke's law of orthotropic anisotropy in Eq. (5) can be reduced to the following form

$$\varepsilon_x = \frac{\sigma_x}{E_x} - \nu_{yx} \frac{\sigma_y}{E_y}, \varepsilon_y = \frac{\sigma_y}{E_y} - \nu_{xy} \frac{\sigma_x}{E_x}, \gamma_{xy} = \frac{\tau_{xy}}{G_{xy}}. \quad (10a-c)$$

Obviously, only four independent material parameters E_x , E_y , G_{xy} and ν_{xy} need to be considered in the scaling relations. When combined with Table 4, the following relation can be found

$$\left(\frac{\beta_{E_y}}{\beta_{E_x}} \right) = \left(\frac{\beta_{G_{xy}}}{\beta_{E_x}} \right)^2 = \left(\frac{1}{\beta_{\nu_{xy}}} \right)^2 = \left(\frac{\beta_{\bar{L}_y}}{\beta_{\bar{L}_x}} \right)^4. \quad (11)$$

In this equation, the similarity of the material parameters is only related to $\beta_{\bar{L}_x}$ and $\beta_{\bar{L}_y}$, not to $\beta_{\bar{L}_z}$. Therefore, the geometric thickness of the structure can be arbitrarily distorted. Nevertheless, it is still difficult to satisfy this equation when different anisotropic materials are used at scaling.

- **The first scheme of the width and thickness distortion**

In order to further relax the restriction of distortion, the dimensionless number of dominant material parameters needs to be further simplified. Firstly, E_x and E_y are assumed to be the dominant material parameters and $E_x \geq E_y$. Then, Eq. (11) can be reduced as

$$\frac{\beta_{\bar{L}_y}}{\beta_{\bar{L}_x}} = \left(\frac{\beta_{E_y}}{\beta_{E_x}} \right)^{1/4} \left(i.e., \beta_{\bar{L}_y} = \left(\frac{\beta_{E_y}}{\beta_{E_x}} \right)^{1/4} \beta_{\bar{L}_x} \right). \quad (12)$$

The above equation shows that the geometric scaling ratio of the two in-plane directions is equal to a quarter power of the scaling ratio of the corresponding material parameters. Therefore, when the scaled model is not the same as the full-size prototype material, the geometric thickness of the structure needs to be corrected to compensate for the material difference.

- **The second scheme of the width and thickness distortion**

In addition, another main distortion method can also be formed when E_x and G_{xy} are assumed as dominant parameters. In this case, Eq. (11) can be reduced as

$$\frac{\beta_{\bar{L}_y}}{\beta_{\bar{L}_x}} = \sqrt{\frac{\beta_{G_{xy}}}{\beta_{E_x}}} \left(i.e., \beta_{\bar{L}_y} = \sqrt{\frac{\beta_{G_{xy}}}{\beta_{E_x}}} \beta_{\bar{L}_x} \right). \quad (13)$$

Compared with the relation in Eq. (12), the ratio of material parameters in Eq. (13) is equal to the ratio of width to length to the 1/2 power. Therefore, different scaling schemes have different width distortion capabilities.

Furthermore, in Eq. (11), $\beta_{\bar{L}_y} = \sqrt{1/\beta_{\nu_{xy}}\beta_{\bar{L}_x}}$ is also an incomplete scaling scheme. However, since the Poisson's ratio is much less important than the effect of elastic modulus on anisotropic thin-plate, this scaling scheme is not desirable, which will be further discussed in depth in Section 4.

From the above analysis, it can be seen that for the case of that the scaled model using the same material as the full-size prototype, only geometric thickness distortion is allowed. For the case of the different materials, except for geometric thickness distortion, the width of the scaled model must be corrected according to Eq. (12) or Eq. (13). The geometric thickness can be corrected to any value without being affected by material parameters, while the correction of geometric width is restricted by the difference of material parameters in the x-y plane. For convenience, the scaling techniques of distortion that fully satisfies Eq. (11), Eq. (12) and Eq. (13) are called the techniques M0, MI and MII, respectively, which are listed in Table 5. In summary, the above derivation establishes the necessary conditions for the similarity of anisotropic elastic materials from the point of view of distortion.

Table 5. Scaling techniques of distortion for anisotropic elasticity in the ODLV system.

Scaling techniques	Dominant parameters	Scaling relation of aspect ratio
M0	E_x, E_y, G_{xy} and ν_{xy}	$\beta_{L_y} = \beta_{L_x}$
M I	E_x and E_y	$\beta_{L_y} = \beta_{L_x} (\beta_{E_y}/\beta_{E_x})^{1/4}$
M II	E_x and G_{xy}	$\beta_{L_y} = \beta_{L_x} (\beta_{G_{xy}}/\beta_{E_x})^{1/2}$

Finally, in addition to the geometry and material needs to meet the distorted scaling requirements, the impact loads also need to be scaled reasonably. According to the scaling relation $\beta_{E_x} = (\beta_\rho \beta_{V_z}^2)(\beta_{L_x}/\beta_{L_z})^4$ in Table 2, the correction of impact velocity can be derived as

$$\beta_{V_z} = \left(\frac{\beta_{L_z}}{\beta_{L_x}} \right)^2 \sqrt{\frac{\beta_{E_x}}{\beta_\rho}}. \quad (14)$$

Equation (14) shows that by correcting the impact velocity, the distortion of geometric thickness and the distortion of materials in density and elasticity modulus can be further compensated. Since β_{V_z} is proportional to $(\beta_{L_z}/\beta_{L_x})^2$, more input energy for scaled model with the case of $\beta_{L_z} > \beta_{L_x}$ is needed to offset the resistance of the structure to deformation caused by the increase in thickness.

3. Verification

In this section, a numerical model of impacted square plate with anisotropic elastic material is used to validate more details of the ODLV's similarity laws of material and geometric distortion from the viewpoints of both spatial and temporal fields.

3.1. A clamped square plate subjected to dynamic pressure pulse

3.1.1. Formulation

To verify the distorted similarity of anisotropic elastic materials, a square plate subjected to transverse dynamic pressure pulse, as shown in Figure 2, is studied. For geometry and load of prototype, $L_p = 100 \text{ mm}$, $B_p = 100 \text{ mm}$, $H_p = 1 \text{ mm}$, $(P_z)_p = 0.2 \text{ MPa}$ and $(t_f)_p = 0.25 \text{ ms}$ are adopted. When the full-size prototype is a thin square plate, according to the proposed scaling technique, it could become a thinner/thicker rectangular plate with unequal length and width after scaling of geometric distortion, as shown in Figure 2a,b. In order to better combine directional similarity framework of ODLV, the dynamic pressure pulse is equivalent to a simple velocity impact in the use of the similarity laws. The load of full-size prototype is approximately equivalent to the impact velocity of $V_0 = 15.8 \text{ m/s}$ by the momentum theorem (i.e., $(P_z LB)t_f/2 = (\rho LBH)V_0$).

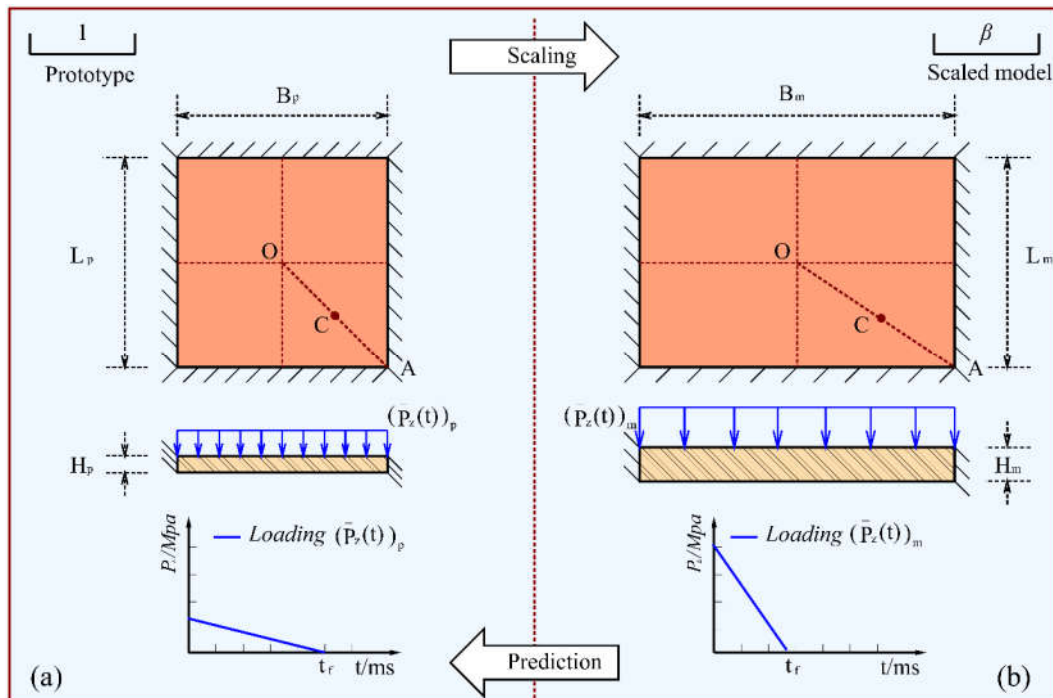


Figure 2. A scaling schematic diagram of a square plate subjected to a transverse dynamic pressure.

To fully verify the proposed scaling techniques, various anisotropic/isotropic materials with different density and the lamina elastic parameters, as shown in Table 6 **Error! Reference source not found.**, are considered. The AS4 is used as the full-size prototype material. For the scaling technique M0, AS4 is also used to make the scaled model. For the scaling technique MI, Virtual material A (VMA), IM7, E-glass and Steel are used to make the scaled model, respectively. For the scaling technique MII, Virtual material B (VMB), IM7, E-glass and Steel are used to make the scaled model, respectively. The VMA and the VMB are two virtual materials in which the material parameters of VMA satisfy Eq. (11) and Eq. (12), and the material parameters of VMB satisfy Eq. (11) and Eq. (13). In addition, the VMA have the same E_{11} and E_{22} with the IM7, so they have the same geometric width distortion when the MI is used. While, the VMB have the same E_{11} and G_{12} with the IM7, as a result, so they have the same geometric width distortion when the MII is used. As a special case, the steel is an isotropic material and satisfied the inherent relation $G = E/2(1 + \nu)$ [32]. As ideal and extreme situations, the virtual and isotropic materials can better test the rationality and applicability of the proposed techniques.

Table 6. Mechanical parameters of materials used for full-size prototype and scaled models.

Materials	ρ [kg/m ³]	E_{11} [GPa]	E_{22} [GPa]	ν_{12} [-]	G_{12} [GPa]	G_{13} [GPa]	G_{23} [GPa]
AS4/epoxy [33]	1580	126	11	0.28	2.60	2.60	3.90
Virtual material A *	1590	162	8.34	0.36	2.57	4.96	4.96
Virtual material B	1590	162	31.12	0.19	4.96	4.96	4.96
IM7/977-3 [34]	1590	162	8.34	0.27	4.96	4.96	4.96
E-glass/epoxy [35]	1780	40	10	0.30	3.15	3.15	4.32
Stainless Steel [36]	8000	193	193	0.30	74.23	74.23	74.23

The clamped square plate prototype with geometry, impact loads and boundary conditions in Figure 2 is modeled by a quarter symmetry model in finite element software using the conventional shell elements and discretized with 100 elements in the direction of length and width. For scaled models, the basic geometric factor β_{L_x} in the direction of the length L is set to 0.1. The basic geometric factor β_{L_y} in the direction of the width B is determined according to Table 5. The basic geometric factor in the thickness direction H is set to 0.05, 0.15, 0.2, 0.3 for the technique M0 and 0.2

for the technique MI and MII. For convenience, the thickness distortion and the width distortion are defined as $\eta_H = \beta_{L_z}/\beta_{L_x}$ and $\eta_B = \beta_{L_y}/\beta_{L_x}$, respectively. For the scaling technique M0, $\eta_H = 0.5, 1.5, 2.0, 3.0$ for four scaled models, respectively. For the scaling technique MI, $\eta_B = 0.88, 0.88, 1.30, 1.84$ for four scaled models, respectively. For the scaling technique MII, $\eta_B = 1.22, 1.22, 1.95, 4.32$ for four scaled models, respectively. Obviously, due to the large difference with full-size prototype in material properties when the isotropic materials are used in the scaled model, large width distortion is more likely to be caused. The basic velocity factor β_{V_z} is determined by Eq. (14). The amplitude and loading time of dynamic pressure pulse are scaled from the full-size prototype by $\beta_{P_z} = \beta_\rho \beta_{V_z}^2$ and $\beta_t = \beta_{L_z}/\beta_{V_z}$ (Table 2), respectively. The scaled models use the same type of element as the full-size prototype and are discretized with 100 elements in the direction of length and $100 \times (\beta_{L_y}/\beta_{L_x})$ elements in the direction of width, respectively. Other settings are completely identical with the full-size prototype in the finite element software. When using the scaling technique M0, MI and MII, scaling factors of the input conditions are listed in Table 7, Table 8 and Table 9, respectively.

Table 7. Scaling factors of input parameters used for scaled models (Scaling technique M0).

Scaled model	β_ρ	β_L	β_B	β_H	β_{V_z}	β_t	β_{P_z}
AS4/epoxy	1.0	0.1	0.1	0.05	0.250	0.200	0.063
AS4/epoxy	1.0	0.1	0.1	0.15	2.250	0.067	5.063
AS4/epoxy	1.0	0.1	0.1	0.2	4.000	0.050	16.000
AS4/epoxy	1.0	0.1	0.1	0.3	9.000	0.033	81.000

Table 8. Scaling factors of input parameters used for scaled models (Scaling technique MI).

Scaled model	β_ρ	β_L	β_B	β_H	β_{V_z}	β_t	β_{P_z}
Virtual material A	1.006	0.1	0.0876	0.2	4.521	0.044	20.571
IM7/977-3	1.006	0.1	0.0876	0.2	4.521	0.044	20.571
E-glass/epoxy	1.127	0.1	0.1301	0.2	2.123	0.094	5.079
Stainless Steel	5.063	0.1	0.1840	0.2	2.200	0.091	24.508

Table 9. Scaling factors of input parameters used for scaled models (Scaling technique MII).

Scaled model	β_ρ	β_L	β_B	β_H	β_{V_z}	β_t	β_{P_z}
Virtual material B	1.006	0.1	0.1218	0.2	4.521	0.044	20.571
IM7/977-3	1.006	0.1	0.1218	0.2	4.521	0.044	20.571
E-glass/epoxy	1.127	0.1	0.1954	0.2	2.123	0.094	5.079
Steel	5.063	0.1	0.4317	0.2	2.200	0.091	24.508

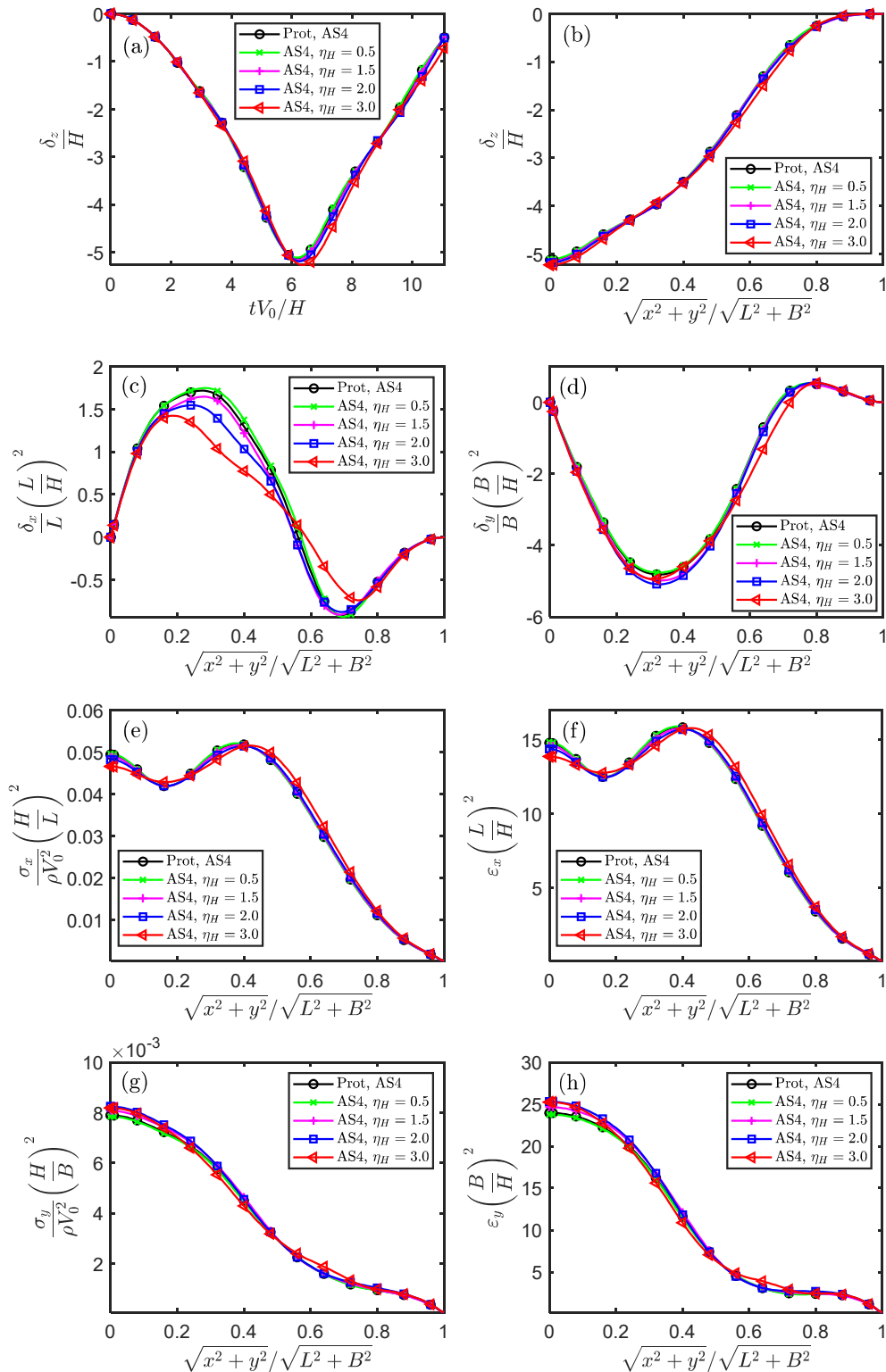
3.1.2. Results analysis

According to the proposed scaling methods, the only thickness distortion, M0, and the simultaneous width and thickness distortion, MI and MII, are analyzed. When the similarity is analyzed from the time fields, the shear stress and shear strain components are taken from the point C (see Figure 2), and the other physical quantities are taken from the point O (see Figure 2). When similarity is analyzed from the space fields, all physical quantities are taken on the diagonal OA (see Figure 2) and in the dimensionless time $tV_0/H = 6.15$. The advantage of using diagonal lines to represent space is that they can comprehensively reflect the similarity results of two main directions of anisotropic materials.

(1) Scaling technique M0: only thickness distortion

For the symmetry square plate with only thickness distortion, the similarity of displacement, stress and strain components is evaluated in the temporal and spatial fields, with the results plotted in Figure 3. For the transverse displacement δ_z , the scaled models always predict the response of the full-size prototype more accurately, Figure 3a,b. For the in-plane displacement δ_x and δ_y , the scaled

models can also better predict the response of the full-size prototype, Figure 3c,d. Some similarity error can be found and it increases with the thickness distortion η_H , especially in Figure 3c. For the stress and strain components in different directions, the scaled models are in good agreement with the full-size prototype, Figure 3e-g. Obviously, when using the scaling technique M0, the scaled model and full-size prototype have good consistency, no matter for stress, strain or displacement components, which is consistent with the analysis results for isotropic plastic materials considering geometric thickness distortion in Ref. [26].



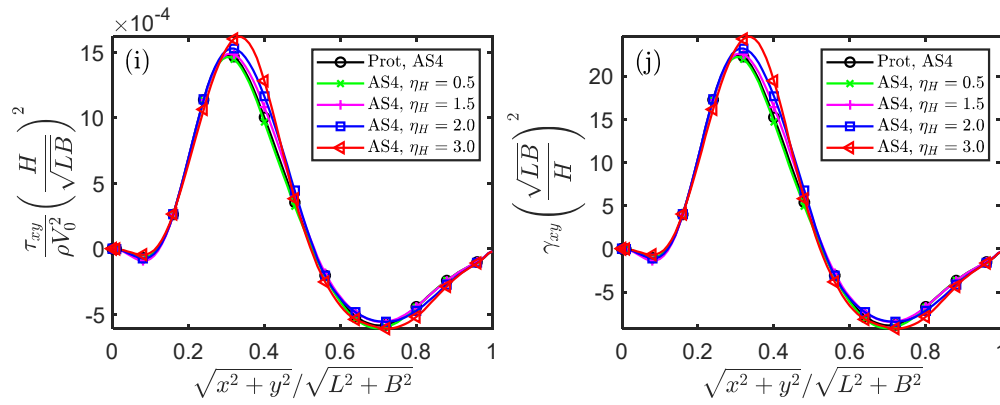


Figure 3. The similarity of displacement, stress and strain components in the temporal and spatial fields for impacted square plate (Scaling technique M0).

When only the geometric thickness distortion is considered, the prediction results of the scaled models are more accurate, but there are still some errors, especially for the large thickness distortion. According to the study of Ref. [26], the increase of similarity error is mainly affected by the increase of rotation angle of neutral plane of scaled model. The scope of application of ODLV is the geometric nonlinearity assumption of the small strains with moderate rotation ($10^\circ - 15^\circ$) of neutral plane [26]. The average rotations for the full-size prototype and the four scaled models respectively estimated as 2.94° , 1.49° , 4.40° , 5.94° and 8.99° , according to the arctangent of $(\delta_z)_{max}/L = 5.13/100$, $0.26/10$, $0.77/10$, $1.04/10$ and $1.58/10$ in Figure 3a. Apparently, with the increase of the geometric thickness of the scaled model, the degree of structural deformation increases significantly, which makes the similarity error increase.

(2) Scaling technique M1: the first scheme of the width and thickness distortion

For the symmetry impact model with width and thickness distortion using the scaling technique M1, the similarity of displacement components is evaluated in the temporal and spatial fields, with the results plotted in Figure 4. For the transverse displacement δ_z , the scaled models always predict the response of the full-size prototype more accurately, whether the model uses the ideal similar material VMA or the vastly different material Steel, Figure 4a and b. For the in-plane displacement δ_x and δ_y , the scaled models can also better predict the response of the full-size prototype, Figure 4c and d. Some significant errors can be observed, especially when the scaled model uses isotropic materials that different greatly from the full-size prototype.

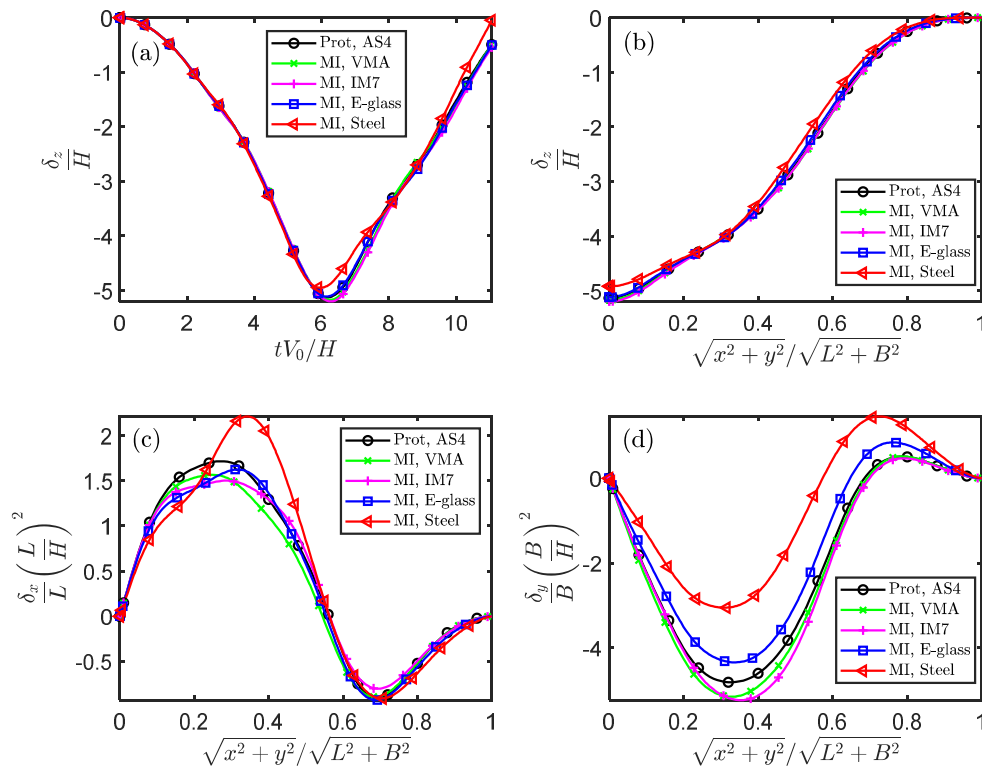
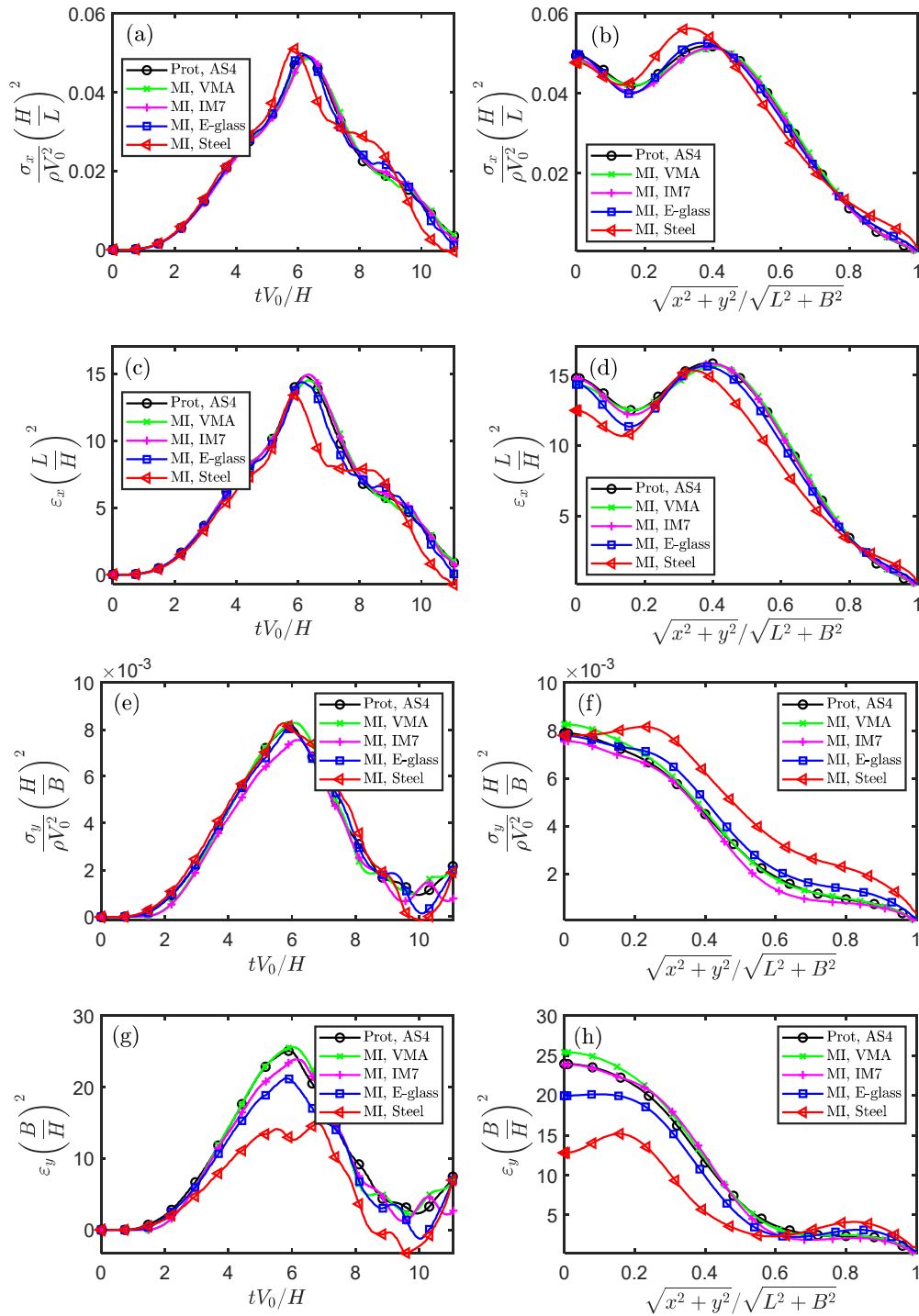


Figure 4. The similarity of displacement components in the temporal and spatial fields for impacted square plate (Scaling technique MI).

The similarity of the stress components and the strain components is further evaluated in the temporal and spatial fields, with the results plotted in Figure 5. For normal stress and normal strain in the x direction, responses between the scaled models and the full-size prototype show good consistency, Figure 5a-d. Although there are some small errors, it becomes significant only when the scaled model is isotropic material Steel. For normal stress and normal strain in the y direction, responses of the scaled models can also better predict those of the full-size prototype, Figure 5e-h. The prediction of the scaled model is accurate when using the material VMA with ideal similarity property, while the errors are significant when using the isotropic steel with large different similarity properties. Since the normal stresses and strains in the x and y directions are basically similar, the scaling technique MI is feasible. However, for the shear stress and shear strain components, the scaled model cannot accurately predict the full-size prototype responses, except for the use of the ideal similar material VMA. The main reason is that the shear modulus G_{xy} cannot meet the requirements of similarity relation Eq. (11), which will be discussed in more depth in Section 4.



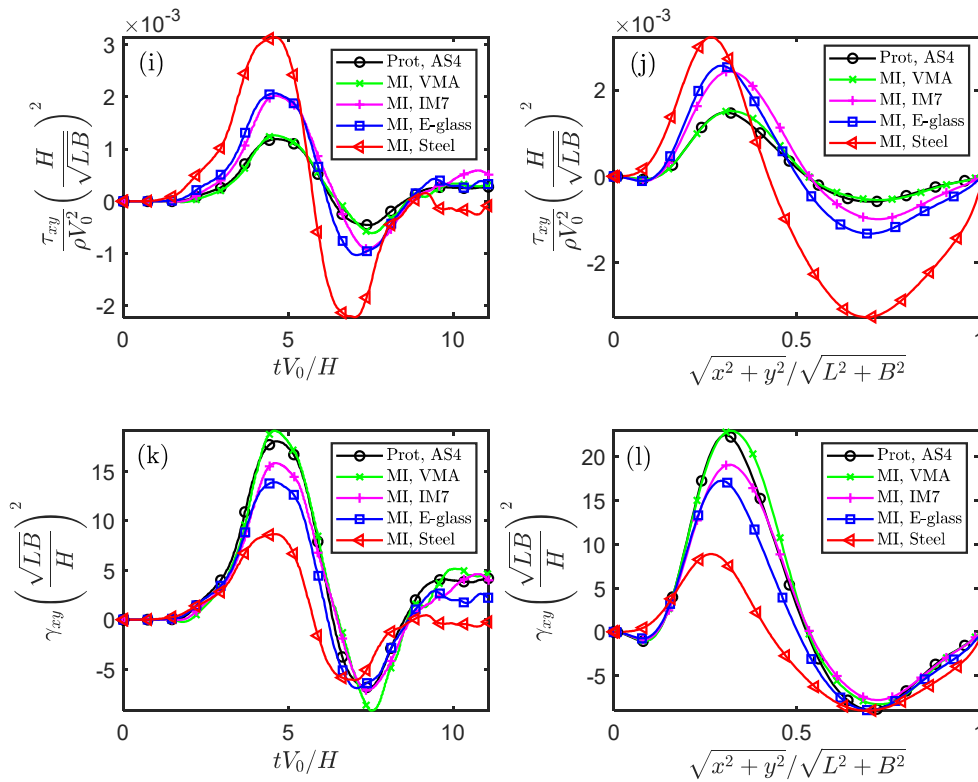


Figure 5. The similarity of stress and strain components in the temporal and spatial fields for impacted square plate (Scaling technique MI).

(3) Scaling technique MII: the second scheme of the width and thickness distortion

For the symmetry impact model with width and thickness distortion using the scaling technique MII, the temporal and spatial similarities of the square plates are shown in Figure 6. It can be seen that except the displacement in the z direction is basically similar, other physical quantities all have very significant similarity errors, unless the material of model is ideal similar material. By contrast, the behavior of the scaled model using ideal similar materials is almost identical to that of the full-size prototype, which further verifies the rationality of the proposed similarity relation of Eq. (11). However, when the scaled model uses isotropic materials, the similarity error between the scaled model and the full-size prototype is the largest. The same phenomenon occurs in the verification of the scaling technique MI, however, the similarity of MI is significantly better than that of MII.

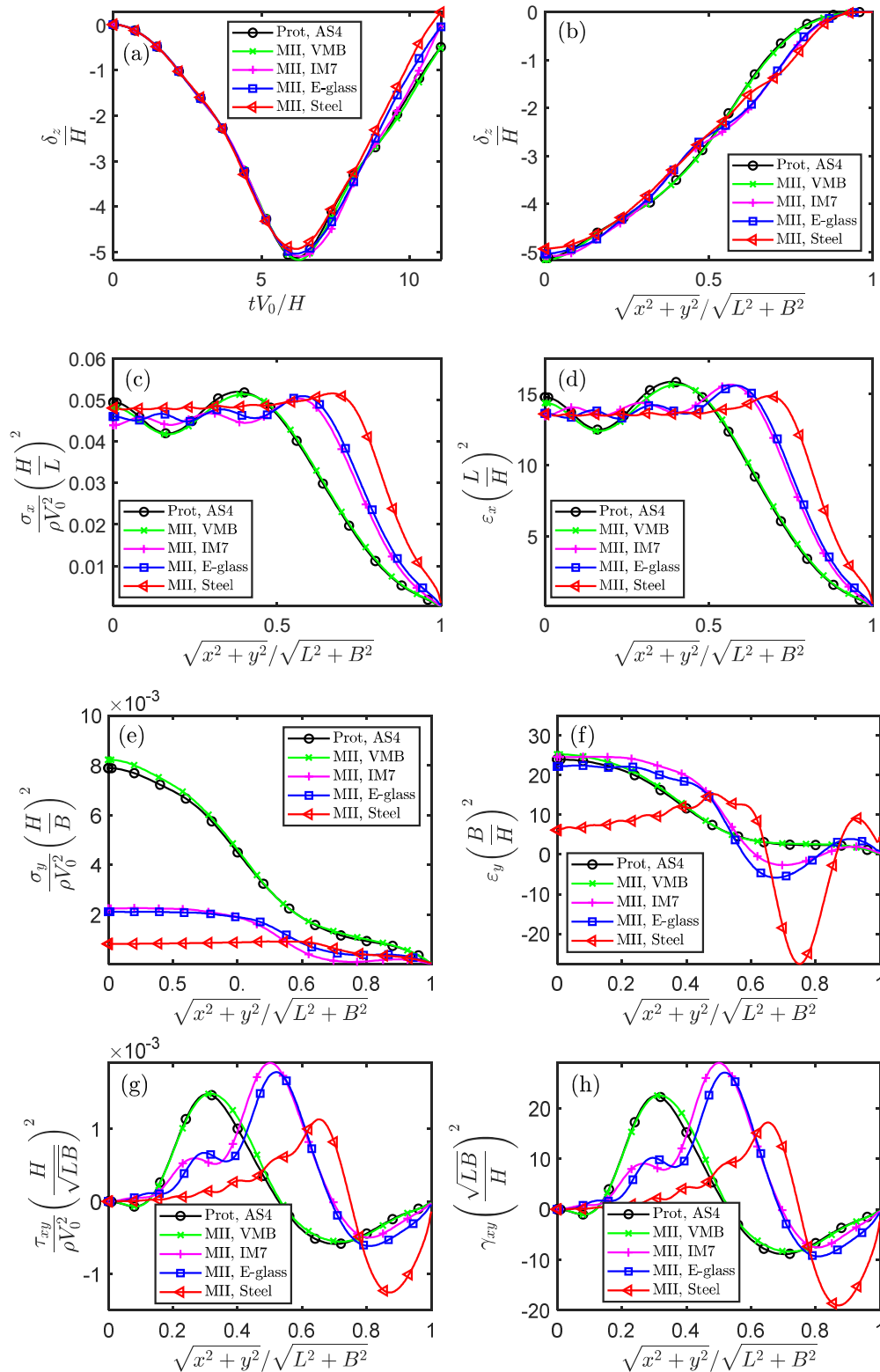


Figure 6. The similarity of displacement, stress and strain components in the temporal fields for impacted square plate (Scaling technique MII).

4. Discussion

When using the distortion methods of geometric thickness and width, the theoretical basis for the establishment of incomplete similarity is the assumption of the relative importance of material parameters. Therefore, it is necessary to discuss the source of similarity error and the importance of these material parameters in depth and to analyze the applicability of incomplete similarity.

(1) The Poisson's ratio ν_{xy} has relatively less effect for similarity.

In the derivation of the incomplete similarity used MI and MII, the Poisson's ratio ν_{xy} is ignored. Based on the Hooke's law of Eq. (10a) and (10b), the influence of the simplification can be discussed by the following two aspects.

Firstly, for the impacted square plate in Section 3.1, the influence of the Poisson's ratio ν_{xy} on the strain ε_x and the strain ε_y is smaller than the influence of E_x and E_y , respectively. To describe the relative importance of the Poisson's ratio, the dimensionless ratios $\xi_x = \left(\nu_{yx} \frac{\sigma_y}{E_y}\right) / \left(\frac{\sigma_x}{E_x}\right)$ and $\xi_y = \left(\nu_{xy} \frac{\sigma_x}{E_x}\right) / \left(\frac{\sigma_y}{E_y}\right)$ are defined from Eq. (10a) and (10b), respectively. Obviously, the greater the value of ξ_x and ξ_y , the greater the contribution of Poisson's ratio on the normal strains. Then, for scaled models used the scaling techniques MI and MII, ξ_x and ξ_y in the spatial fields are plotted in Figure 7. Since the y-coordinate of the curve is less than 1, the contribution of $\left(\nu_{yx} \frac{\sigma_y}{E_y}\right)$ for ε_x and the contribution of $\left(\nu_{xy} \frac{\sigma_x}{E_x}\right)$ for ε_y are significantly less than those of $\left(\frac{\sigma_x}{E_x}\right)$ and $\left(\frac{\sigma_y}{E_y}\right)$, respectively. Therefore, it is reasonable to ignore the Poisson's ratio ν_{xy} but keep parameters E_x , E_y and G_{xy} when selecting the dominant similarity parameters. In addition, it can be found that the value of ξ_y is, on the whole, much greater than that of ξ_x . Thus, the Poisson's ratio does more damage to similarity in the y direction than in the x direction, which is consistent with the similarity analysis in Section 3.1.2.

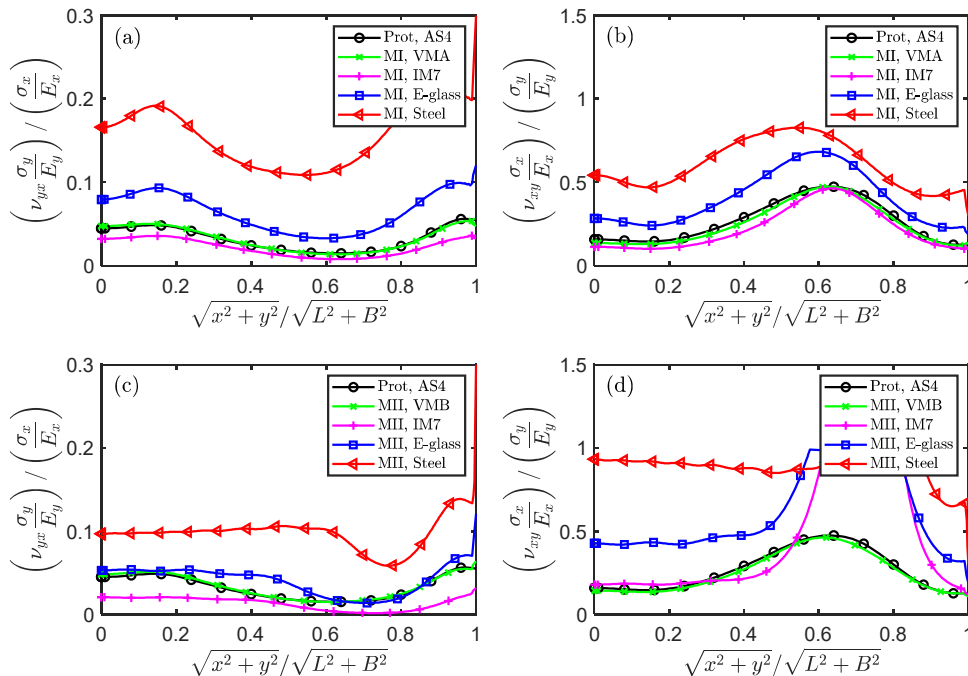


Figure 7. The ratio of the normal strain components caused by stress in the x and y directions for impacted square plate (Scaling techniques MI and MII).

Secondly, the more significant difference between Poisson's ratio and its ideal similar value, the greater the similarity error in the x and y directions. According to Eq. (11), the ideal similar value of ν_{xy} is defined as $\nu_{xy}^{ideal} = (\nu_{xy})_p \left(\beta_{L_x}/\beta_{L_y}\right)^2$. The relative difference of ν_{xy} to ν_{xy}^{ideal} is defined as

$\eta_{v_{xy}} = (v_{xy})_m / v_{xy}^{ideal} = \beta_{v_{xy}} (\beta_{L_y} / \beta_{L_x})^2$. It is also easy to prove that $\eta_{v_{xy}} = (\xi_x)_m / (\xi_x)_p$. Therefore, when $\eta_{v_{xy}} = 1$, there is no error between the scaled model and the full-size prototype; when the absolute value of $\eta_{v_{xy}}$ gets further away from 1, the scaled model deviates more from the full-size prototype. For the scaling techniques MI, $\eta_{v_{xy}} = 1, 0.7, 1.8, 3.6$ for VMA, IM7, E-glass and Steel, respectively. For the scaling techniques MII, $\eta_{v_{xy}} = 1, 1.4, 4.1$ and 20.0 for VMB, IM7, E-glass and Steel, respectively. Obviously, the scaled model made of Steel has the largest deviation from the full-size prototype, while VMA/VMB has the smallest deviation. This explains why the scaled models of some materials have good similarity and others have poor similarity when using the scaling techniques MI and MII.

In order to further quantitatively explore the similarity error caused by $\eta_{v_{xy}}$, the materials VMA and VMB with six new hypothetical Poisson's ratio in Table 10 are further used. The scaling factors and numerical models are exactly the same as 'MI (VMA)' and 'MII (VMB)' in Section 3.1.1, except for Poisson's ratio. When $\eta_{v_{xy}}$ increases from 1/4 to 4, the average error of strain components ε_x , ε_y and γ_{xy} on the time field is shown in Figure 8. It can be seen that when the scaling techniques MI and MII are used, the similarity error is almost consistent with the change of $\eta_{v_{xy}}$. When $\eta_{v_{xy}} < 1$, the average error of strain components in the x, y and x-y directions are all about 5%, showing good similarity. Combined with Figure 7, the main reason is that the Poisson's ratio contributes less to strain component in both full-size prototype and scaled models. However, when $\eta_{v_{xy}} > 1$, the average error increases significantly as $\eta_{v_{xy}}$ increases. In this case, the strain component ε_y has the largest similarity error (about 10 % and 25% for $\eta_{v_{xy}} = 2$ and 4, respectively), while ε_x has the smallest similarity error (about 10% for $\eta_{v_{xy}} = 4$). Therefore, by designing optimal similarity material to control the value of $\eta_{v_{xy}}$ (such as $\eta_{v_{xy}} < 2$), the similarity loss caused by Poisson's ratio can be significantly reduced.

Table 10. Hypothetical parameter of Poisson's ratio for the material VMA and VMB.

$\eta_{v_{xy}}$	1/4	1/3	1/2	1	2	3	4
$(v_{12})_{VMA}$	0.09	0.12	0.18	0.36	0.72	1.08	1.44
$(v_{12})_{VMB}$	0.0475	0.063	0.095	0.19	0.38	0.57	0.76

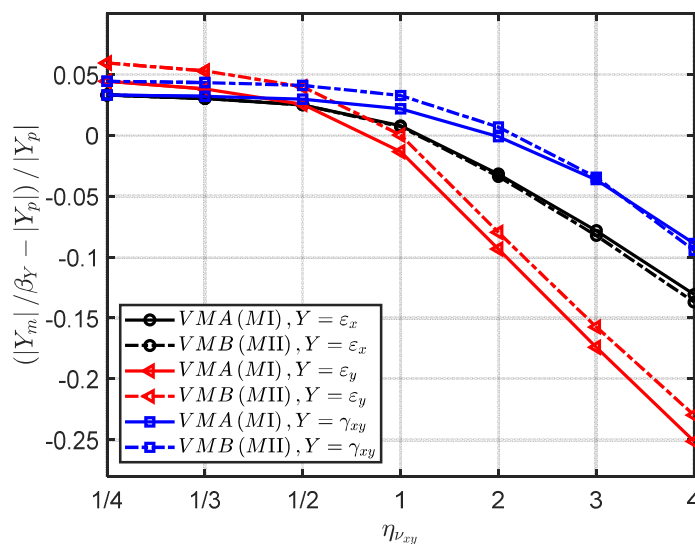


Figure 8. The similarity error of strain components as $\eta_{v_{xy}}$ changes (Scaling techniques MI and MII).

(2) Ignoring the shear modulus G_x or the elasticity modulus E_y easily break similarity.

In the derivation of the scaling technique MI, another important reason for breaking the complete similarity is that the shear modulus G_{xy} is ignored. While, on the derivation of the scaling

technique MII, the elasticity modulus E_y is ignored. According to Eq. (11), the ideal similar value of G_{xy} and E_y are defined as $G_{xy}^{ideal} = (G_{xy})_p \beta_{E_x} (\beta_{L_y} / \beta_{L_x})^2$ and $E_y^{ideal} = (E_y)_p \beta_{E_x} (\beta_{L_y} / \beta_{L_x})^4$, respectively. The ratio of G_{xy} to G_{xy}^{ideal} and the ratio of E_y to E_y^{ideal} are expressed as $\eta_{G_{xy}} = (G_{xy})_m / G_{xy}^{ideal} = (\beta_{G_{xy}} / \beta_{E_x}) (\beta_{L_x} / \beta_{L_y})^2$ and $\eta_{E_y} = (E_y)_m / E_y^{ideal} = (\beta_{E_y} / \beta_{E_x}) (\beta_{L_x} / \beta_{L_y})^4$, respectively. For VMA, IM7, E-glass and Steel in the scaling technique MI, $\eta_{G_{xy}} = 1, 1.9, 2.3$ and 5.5 , respectively. For VMB, IM7, E-glass and Steel in the scaling technique MII, $\eta_{E_y} = 1, 0.27, 0.20$ and 0.03 , respectively. Obviously, except for the virtual material, $\eta_{G_{xy}}$ and η_{E_y} of other materials are very different from their corresponding ideal values, especially for the isotropic Steel. When combined with Figures 5i-l and 6, it can be found that these differences are consistent with the error of the full-size prototype predicted by the scaled model. The above also analysis explains why the similarity errors increase significantly when isotropic Steel different from properties of the full-size prototype is selected for the scaled model. Therefore, better similarity can be obtained for materials with MI whose design parameter G_{xy} is close to G_{xy}^{ideal} and for materials with MII whose design parameter E_y is close to E_y^{ideal} .

In order to further quantitatively explore the similarity error caused by $\eta_{G_{xy}}$, the materials VMA with hypothetical shear modulus in Table 11 are further used. The scaling factors and numerical models are exactly the same as 'MI (VMA)' in Section 3.1.1, except for shear modulus. When $\eta_{G_{xy}}$ increases from 1/4 to 4, the average error of strain components ε_x , ε_y and γ_{xy} on the time field is shown in Figure 9. It can be seen that, when the absolute value of $\eta_{G_{xy}}$ gets further away from 1, the average error of the strain ε_x and γ_{xy} increases significantly, while the average error of the strain ε_y remains almost zero. In contrast, at the same distance, the similarity error is larger when $\eta_{G_{xy}} > 1$ than when $\eta_{G_{xy}} < 1$. In this case, the strain γ_{xy} has the largest similarity error, even reaching 36% for $\eta_{G_{xy}} = 4$. Therefore, by designing optimal similarity material to control the value of $\eta_{G_{xy}}$ (such as $1/2 < \eta_{G_{xy}} < 2$), the similarity loss caused by shear modulus can be significantly reduced.

Table 11. Hypothetical parameter of shear modulus for the material VMA.

$\eta_{G_{xy}}$	1/4	1/3	1/2	1	2	3	4
$(G_{12})_{VMA}[\text{GPa}]$	0.643	0.857	1.285	2.57	5.14	7.71	10.28

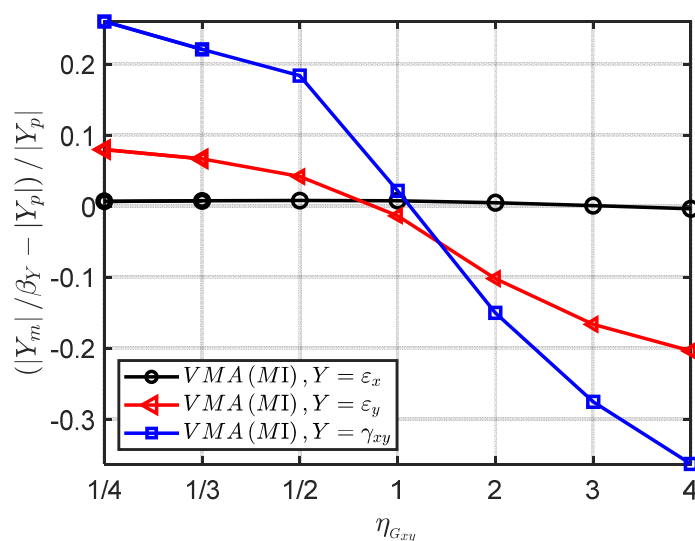


Figure 9. The similarity error of strain components as $\eta_{G_{xy}}$ changes (Scaling techniques MI).

In order to further quantitatively explore the similarity error caused by η_{E_y} , the materials VMB with hypothetical elastic modulus in Table 12 are further used. The scaling factors and numerical

models are exactly the same as 'MII (VMB)' in Section 3.1.1, except for the elastic modulus in the y direction. When η_{E_y} increases from 1/4 to 4, the average error of strain components ε_x , ε_y and γ_{xy} on the time field is shown in Figure 10. It can be seen that, when the absolute value of η_{E_y} gets further away from 1, the average error of the strain ε_x and γ_{xy} increases significantly, while the average error of the strain ε_y is smaller. In contrast, the strain γ_{xy} has the largest similarity error, even reaching 62% for $\eta_{E_y} = 1/4$. Therefore, by designing optimal similarity material to control the value of η_{E_y} (such as $3/4 < \eta_{E_y} < 2$), the similarity loss caused by shear modulus can be significantly reduced.

Table 12. Hypothetical parameters of elastic modulus for the material VMB.

η_{E_y}	1/4	1/3	1/2	1	2	3	4
$(E_{22})_{VMB}$ [GPa]	7.78	10.37	15.56	31.12	62.24	93.36	124.48

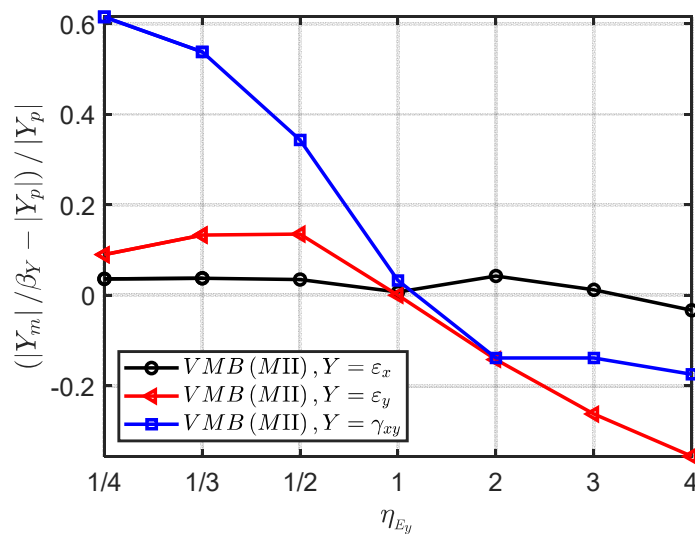


Figure 10. The similarity error of strain components as η_{E_y} changes (Scaling technique MII).

(3) The technique MI is easier to get good similarity.

In the results analysis in Section 3.1.2, the similarity of MI is significantly better than that of MII. For IM7, E-glass and Steel, $(\eta_B)_{MII}/(\eta_B)_{MI} = 1.39, 1.50, 2.35$ and $(\eta_{v_{xy}})_{MII}/(\eta_{v_{xy}})_{MI} = 1.3, 3.9, 7.3$, respectively. In terms of the Poisson's ratio $\eta_{v_{xy}}$, the scaling technique MII has a larger geometric width distortion capacity and therefore causes greater damage to similarity of the impact plates in Figure 2. The main reason for this phenomenon is that the width distortion of the technique MII is proportional to the 1/2 power of material parameter ratio rather than the 1/4 power of the technique MI. Therefore, the width distortion of the method MII is more sensitive to the value of material parameter ratio and more likely to cause serious distortion. This difference can be further verified by the values of $\eta_{G_{xy}}$ and η_{E_y} . When the technique MII is used for IM7, E-glass and Steel, the difference between E_y and E_y^{ideal} is intuitively greater than that between G_{xy} and G_{xy}^{ideal} , which may also lead to greater similarity error.

In addition, another potential advantage of using the technique MI over the technique MII is when scaled model and full-size prototype use different isotropic elastic materials. In this case, the technique MI naturally degenerates into the geometric similarity with $\beta_{L_y} = \beta_{L_x}$, while the technique MII may still maintain the width distortion $\beta_{L_y} \neq \beta_{L_x}$ if $\nu_m \neq \nu_p$. This means that use of the technique MII will lose some similarity due to width distortion. Recall that, Ref. [28] takes the stiffness coefficients in the x direction and the x-y plane as the dominant material parameters at incomplete similarity of anisotropic elasticity, which is similar to the scaling technique MII in this paper. The

above analysis also indicates that compared with Ref. [28], the scaling technique MI proposed in this paper have better similarity.

5. Conclusions

This paper presents a distortion similarity laws that relates full-size prototype and scaled model made of same or different anisotropic elasticity materials. In order to explore this method, the recently developed directional similarity law framework (termed as ODLV) are extended by further considering the orthotropic Hooke's law. The characteristic length of three spatial directions replaces the traditional single scalar characteristic length to express similarity laws of anisotropic elasticity materials, and the correction techniques of the geometric width and thickness of the structure are proposed to overcome the inherent distortion problems of the previous similarity laws. Four are the main aspects in the method outlined here.

(1) Based on the oriented dimensional analysis method and the thin-plate impact model, oriented dimensions, directional dimensionless numbers and directional scaling relations of the elastic modulus and the Poisson's ratio of anisotropic materials are comprehensively proposed. Compared with the previous scalar dimensional analysis, the directional dimensionless number and directional scaling relation proposed in this paper can effectively express the directivity of geometric space and anisotropic material parameters, which lays a foundation for breaking the limitation of the scaling of material and geometric distortion of anisotropic elasticity.

(2) In order to obtain material and geometric distortion of anisotropic elasticity, three important scaling techniques with correction of width and thickness are further proposed based on the proposed directional scaling relations. Firstly, by ignoring the influence of transverse material parameters, the scaling technique M0 with four dominant similar parameters E_x , E_y , G_{xy} and ν_{xy} is proposed. In this case, the scaling relation of the in-plane material parameters is independent of the thickness direction, allowing arbitrary thickness distortion when same anisotropic elastic materials are used for scaled model and full-size prototype. Secondly, the scaling technique MI with dominant similar parameters E_x and E_y and the scaling technique MII with dominant similar parameters E_x and G_{xy} are proposed to further consider distortion case of different anisotropic elastic materials. In the two cases, the geometric width of the scaled model needs to be further reasonably corrected to compensate for the difference in material properties in the x-y plane. This also means that a square plate will be scaled to a thicker/thinner rectangular plate, or a circular plate will be scaled to a thicker/thinner elliptical plate.

(3) The similarity of different anisotropic and isotropic materials is validated by the numerical impact model of a clamped thin square plate subjected to transverse impulse pressure. The results show that when scaling technique M0 is used, all kinds of responses of displacement, stress and strain components on the thin square plate are almost consistent with the full-size prototype on the thicker square plate. When the scaling technique MI is used, the thin square plate is distorted into a rectangular square plate, and the various responses in the x and y directions are consistent with the full-size prototype, while the responses in the x-y direction are significantly different from the full-size prototype. When the scaling technique MII is used, only the transverse displacement is similar, while the responses in other directions have significant errors with the full-size prototype.

(4) The selection criterion of anisotropic material parameters to obtain optimal similarity are analyzed in depth and the applicability of the proposed methods are discussed. The results show that for the thickness distortion of anisotropic elastic materials, the similarity error increases slightly with the increase of the distortion degree. Under the applicable condition of geometric nonlinearity of the ODLV system (i.e., the small strains with moderate rotation (10° - 15°) of neutral plane), the scaled model and the full-size prototype has a good similarity. For the width distortion of anisotropic elastic materials, the Poisson's ratio ν_{xy} is not the dominant similar parameter because its influence is not as significant as that of elastic modulus at scaling. The in-plane shear modulus G_{xy} and elastic modulus E_y are the main causes of similarity error. The greater the difference between their values and ideal similar values, the greater the similarity error. In order to obtain good similarity, the materials of scaled model should be designed as close to the ideal similar value as possible. The

scaling technique MI could have better similarity than the scaling technique MII, which is mainly due to stronger ability of width distortion in the technique MII, resulting in greater loss of similarity.

Since the proposed similarity laws of anisotropic elastic materials in this paper is limited to the thin-plate impact plate with monolayer anisotropic elastic material, it is necessary to further study for the more complex anisotropic impact problem.

Authorship Roles: Shuai Wang: Conceptualization, Methodology, Formal analysis, Writing - original draft, Software, Investigation; Xinzhe Chang: Writing - review & editing, Software, Validation; Fei Xu: Supervision, Methodology, Writing - review & editing, Resources, Funding acquisition; Jicheng Li: Validation; Jiayi Wang: Validation.

Acknowledgements: This work is supported by the National Nature Science Foundations of China [grant no. 11972309 and grant no. 12072333] and the Overseas Expertise Introduction Project for Discipline Innovation (the 111 Project) [grant no. BP0719007].

Declaration of Competing Interest: The authors declare that they have no known competing financial interests or personal relationships that could have appeared to influence the work reported in this paper.

References

1. Jones, N., 1989. Structural impact. Cambridge University Press, Cambridge.
2. Lu, G., Yu, T.X., 2003. Energy absorption of structures and materials. Cambridge Woodhead Publishing, Cambridge.
3. Coutinho, C.P., Baptista, A.J., Rodrigues, J.D., 2016. Reduced scale models based on similitude theory: A review up to 2015. *Engineering Struct.*, 119, 81–94. <http://dx.doi.org/10.1016/j.engstruct.2016.04.016>
4. Casaburo, A., Petrone, P., Franco, F., Rosa, S.D., 2019. A Review of Similitude Methods for Structural Engineering. *Appl. Mech. Rev.*, 71(3): 030802. <https://doi.org/10.1115/1.4043787>
5. J. Morton, 1988. Scaling of impact-loaded carbon-fiber composites. *AIAA J.*, 26, 989-994.
6. Sutherland, L.S., Guedes Soares, C., 2007. Scaling of impact on low fibre-volume glass-polyester laminates. *Compos. Part Appl. Sci. Manuf.* 38(2), 307–317. <https://doi.org/10.1016/j.compositesa.2006.04.003>
7. F.J. Yang, M.Z. Hassan, W.J. Cantwell, N. Jones, 2013. Scaling effects in the low velocity impact response of sandwich structures. *Compos. Struct.*, 99, 97–104. <https://doi.org/10.1016/j.compstruct.2012.11.011>
8. Z. Xu, F. Yang, Z.W. Guan, W.J. Cantwell, 2016. An experimental and numerical study on scaling effects in the low velocity impact response of CFRP laminates. *Compos. Struct.*, 156, 69-78. <https://doi.org/10.1016/j.compstruct.2016.07.029>
9. J., Rezaeepazhand, G.J., Simiteses, J.H., Starnes Jr., 1996. Scale models for laminated cylindrical shells subjected to axial compression. *Composite Structures*, 34(4): 371-379. [https://doi.org/10.1016/0263-8223\(95\)00154-9](https://doi.org/10.1016/0263-8223(95)00154-9)
10. Jones, N., Jouri, W. and Birch, R., 1984. On the scaling of ship collision damage, *International Maritime Association of the East Mediterranean, Third International Congress on Marine Technology, Athens, 2*, 287–94.
11. Jiang, P., Wang, W., Zhang, G.J., 2006. Size effects in the axial tearing of circular tubes during quasi-static and impact loadings. *Int. J. Impact Eng.* 32, 2048-2065. <https://doi.org/10.1016/j.ijimpeng.2005.07.001>
12. Fu, S., Gao, X., Chen, X., 2018. The similarity law and its verification of cylindrical lattice shell model under internal explosion. *Int. J. Impact Eng.* 122, 38–49. <https://doi.org/10.1016/j.ijimpeng.2018.08.010>
13. Drazetic, P., Ravalard, Y., Dacheux, F., Marguet, B., 1994. Applying non-direct similitude technique to the dynamic bending collapse of rectangular section tubes. *Int. J. Impact Eng.* 15, 797–814. [https://doi.org/10.1016/0734-743X\(94\)90066-T](https://doi.org/10.1016/0734-743X(94)90066-T)
14. Oshiro, R.E., Alves, M., 2004. Scaling impacted structures. *Arch. Appl. Mech.* 74, 130–145. <https://doi.org/10.1007/s00419-004-0343-8>
15. Mazzariol, L.M., Oshiro, R.E., Alves, M., 2016. A method to represent impacted structures using scaled models made of different materials. *Int. J. Impact Eng.* 90, 81-94. <https://doi.org/10.1016/j.ijimpeng.2015.11.018>
16. Sadeghi, H., Davey, K., Darvizeh, R., Darvizeh, A., 2019. A scaled framework for strain rate sensitive structures subjected to high rate impact loading. *Int. J. Impact Eng.* 125, 229-245. <https://doi.org/10.1016/j.ijimpeng.2018.11.008>
17. Sadeghi, H., Davey, K., Darvizeh, R., Darvizeh, A., 2019. Scaled models for failure under impact loading. *Int. J. Impact Eng.* 129, 36-56. <https://doi.org/10.1016/j.ijimpeng.2019.02.010>
18. Wang, S., Xu, F., Dai, Z., 2020. Suggestion of the DLV dimensionless number system to represent the scaled behavior of structures under impact loads. *Arch. Appl. Mech.* 90, 707-719. <https://doi.org/10.1007/s00419-019-01635-9>

19. Wang, S., Xu, F., Dai, Z., et al., 2020. A direct scaling method for the distortion problems of structural impact. *Chinese Journal of Theoretical and Applied Mechanics*. 52, 774-786 (in Chinese). <https://doi.org/10.6052/0459-1879-19-327>
20. Wang, S., Xu, F., Zhang, X., Yang, L., Liu, X., 2021. Material similarity of scaled models. *Int. J. Impact Eng.* 156, 103951. <https://doi.org/10.1016/j.ijimpeng.2021.103951>
21. Oshiro, R.E., Alves, M., 2012. Predicting the behaviour of structures under impact loads using geometrically distorted scaled models. *J. Mech. Phys. Solids* 60, 1330-1349. <https://doi.org/10.1016/j.jmps.2012.03.005>
22. Zhong, Y., Jiang, Z., Yao, X., Shi, K., Luo, B., 2018. Impact comparability rule for single layer reticulated shells considering effects of geometric deviation and gravity. *Journal of Vibration and Shock*. 3(37), 230-236. (in Chinese) <https://doi.org/10.13465/j.cnki.jvs.2018.03.036>
23. H., Kang, X., Guo, Q., Zhang, H., Cui, S., Wang, W., Yan., 2021. Predicting the behavior of armored plates under shallow-buried landmine explosion using incomplete scaling models. *Int. J. Impact Eng.* 156, 103970. <https://doi.org/10.1016/j.ijimpeng.2021.103970>
24. Mazzariol, L.M., Alves, M., 2019. Similarity laws of structures under impact load: Geometric and material distortion. *Int. J. Mech. Sci.* 157-158, 633-647. <https://doi.org/10.1016/j.ijmecsci.2019.05.011>
25. Autar K. Kaw., 2006. *Mechanics of composite materials*. Taylor & Francis.
26. Wang, S., Xu, F., Zhang, X., Dai, Z., X. Liu, C., Bai, 2022. A directional framework of similarity laws for geometrically distorted structures subjected to impact loads. *Int. J. Impact Eng.* 161, 104092. <https://doi.org/10.1016/j.ijimpeng.2021.104092>
27. Li X., Xu F., Yang L., Wang S., Liu X., Xi X., Liu J., 2021. Study on the similarity of elasticity and ideal plasticity response of thin plate under impact loading. *Explosion And Shock Waves*, 41(11): 113103. (in Chinese) <https://doi.org/10.11883/bzycj-2020-0374>
28. Davey, K., Darvizeh, R., Golbaf, A., Sadeghi, H., 2020. The breaking of geometric similarity. *Int. J. Mech. Sci.* 187, 105925. <https://doi.org/10.1016/j.ijmecsci.2020.105925>
29. Zhao, Y.P., 1998. Prediction of structural dynamic plastic shear failure by Johnson's damage number. *Forsch. Ingenieurwes.* 63, 349-352. <https://doi.org/10.1007/PL00010753>
30. Huntley, H.E., 1952. *Dimensional analysis*. MacDonald & Co. Ltd., London.
31. Chien W.Z., 1993. *Applied mathematics*. Anhui Science and Technology Press, Hefei. (in Chinese)
32. Reddy, J.N., 2007. *Theory and analysis of elastic plates and shells (Second Edition)*. CRC Press ; Taylor & Francis Group.
33. A., Schiffer, W.J., Cantwell, V.L., Tagarielli, 2015. An analytical model of the dynamic response of circular composite plates to high-velocity impact. *Int. J. Impact Eng.* 85, 67-82. <https://doi.org/10.1016/j.ijimpeng.2015.06.010>
34. J., Zhang, X., Zhang, 2015. An efficient approach for predicting low-velocity impact force and damage in composite laminates. *Compos. Struct.* 130, 85-94. <https://doi.org/10.1016/j.compstruct.2015.04.023>
35. H., Singh, K.K., Namala, P., Mahajan, 2015. A damage evolution study of E-glass/epoxy composite under low velocity impact. *Compos. Part B-Eng.* 76, 235-248. <https://doi.org/10.1016/j.compositesb.2015.02.016>
36. William, D., Callister, Jr., 2007. *Materials science and engineering: an introduction*. John Wiley & Sons.

Disclaimer/Publisher's Note: The statements, opinions and data contained in all publications are solely those of the individual author(s) and contributor(s) and not of MDPI and/or the editor(s). MDPI and/or the editor(s) disclaim responsibility for any injury to people or property resulting from any ideas, methods, instructions or products referred to in the content.